Material Matters™

Chemistry Driving Performance

ALDRICH®

Hydrogen Storage Materials

System Targets for
On-Board Vehicular
H_2 Storage—U.S. DOE

Dehydrogenation of
Ammonia Borane

Metal Borohydrides
for H_2 Storage

Mechanical Processing
in H_2 Storage

Protective Nanocoatings
for Metal Hydrides

Organic Liquid
Storage of Hydrogen

Gas Sorption
Analysis Tool

Solid-State NMR of
Metal Hydrides

Hydrogen—the clean and safe fuel of the future.

SIGMA-ALDRICH

Introduction

Introduction

For more than a decade, hydrogen as an alternative to traditional energy sources such as oil and natural gas has been the focus of research and development efforts in all technologically advanced countries of the world. It is strongly believed that hydrogen can help to address the growing demand for energy and slow down global climate change. In fact, hydrogen can be produced from a variety of sources including fossil fuels, renewables and water (by means of nuclear, wind or solar energy). It is non-toxic and, as an energy carrier, extremely environmentally benign since water is the only exhaust product when hydrogen is converted into energy.

Despite obvious benefits, an immediate incorporation of hydrogen into the world economy faces a number of challenges. Unlike oil and natural gas, hydrogen has no large-scale infrastructure supporting its transportation. Although it is routinely used by chemical and refining industries, the cost of hydrogen storage and delivery is too high for many energy applications, thus impeding the introduction of the Hydrogen Economy in which energy is stored and transported using hydrogen as a major energy carrier.

The Hydrogen Economy Infrastructure is comprised of five key elements—Production, Delivery, Storage, Conversion, and Applications—which are in different stages of technological advancement.
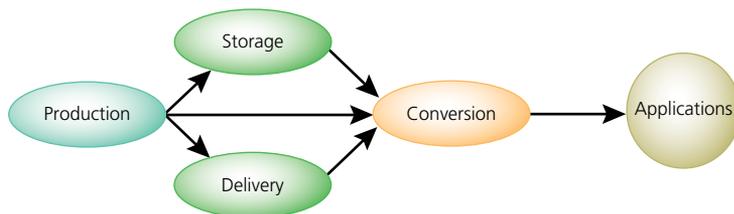
While hydrogen production and conversion are already technologically feasible, its delivery and storage face serious challenges. For example, due to possible hydrogen embrittlement of steel, existing natural gas transmission systems may be unsuitable for the transportation of pure hydrogen gas. Therefore, other options, such as blending with natural gas, a compressed gas or cryogenic liquid delivery as well as alternative hydrogen carriers (methanol, ethanol, and other organic liquids), are being considered. Currently, none of the options in the market satisfy the needs of end users, which explains the growing interest and investment in hydrogen energy related research and development.

Materials-based approaches to hydrogen storage using ammonia borane, hydrides, amides, composite materials, metal-organic frameworks, organic molecules, etc. are being explored extensively. In this thematic issue of *Material Matters*™, the state-of-the-art in hydrogen storage is presented. Leading experts from the U.S. Department of Energy, the Pacific Northwest National Laboratory, General Electric Global Research, Sigma-Aldrich, Louisiana Tech University, Asemblon, Inc., Hy-Energy, Inc., and the California Institute of Technology discuss key aspects of hydrogen storage technologies from goals and targets, materials and processing, to performance evaluation and characterization techniques.

Also featured are Sigma-Aldrich products designed to accelerate your research to advance the Hydrogen Economy. We invite your comments, questions and suggestions about *Material Matters*™ and materials of interest to you: **matsci@sial.com**.

Viktor Balema, Ph.D.
Materials Science
Sigma-Aldrich Corporation

About Our Cover

Safe and environmentally friendly storage of hydrogen contributes a major challenge for a viable Hydrogen Economy. Regardless of the way in which the Hydrogen Economy is implemented, storing hydrogen on-board a vehicle—a car, an aircraft or a ship—is crucial for its realization. Solids are among the safest and most efficient media capable of storing significant amounts of hydrogen and releasing it upon demand. Our cover illustrates a schematic of a solid hydrogen storage material and possible applications on land, sea, and in space.

Portion of the cover image was adapted from "Hydrogen Storage." *MRS Bulletin* **Vol. 27, No. 9 (2002) Reproduced by permission of the** *MRS Bulletin*.

ALDRICH®

U.S. Department of Energy's System Targets for On-Board Vehicular Hydrogen Storage
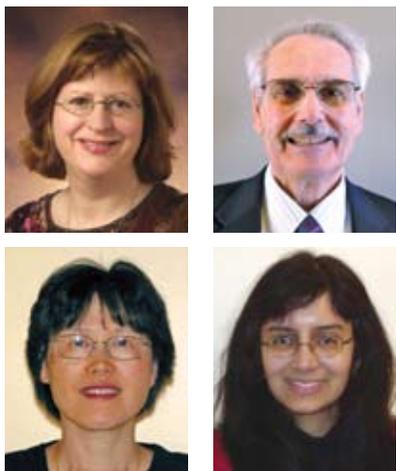
Dr. Carole Read, Dr. George Thomas,
Ms. Grace Ordaz, and Dr. Sunita Satyapal*
U.S. Department of Energy, Hydrogen Program

Introduction

The performance of hydrogen fuel cell vehicles must be comparable or superior to today's gasoline vehicles in order to achieve widespread commercial success. In the North American market, an on-board hydrogen storage technology that allows a driving range of more than 300 miles is critical to meet consumer requirements for most light-duty vehicles. By translating vehicle performance requirements into storage system needs, DOE has described technical targets for 2010 and 2015. These targets are based on equivalency to current gasoline storage systems in terms of weight, volume, cost, and other operating parameters. The DOE hydrogen storage system targets help guide researchers by defining system requirements in order to achieve commercially viable hydrogen storage technologies.

On-Board Vehicular Hydrogen Storage Targets

On-board vehicular hydrogen storage system performance targets were developed by the DOE through the FreedomCAR & Fuel Partnership.[1] These performance targets are application driven, based on achieving similar performance and cost specifications as commercially available gasoline storage systems for light-duty vehicles. The storage system includes all of the hardware (e.g. tank, valves, regulators, piping, mounting brackets, insulation, added cooling capacity, thermal management and any other balance-of-plant components) in addition to any storage media and a full charge of hydrogen.

Table 1 shows a subset of the DOE hydrogen storage system targets for 2010.[2–4] The 2010 targets would allow some vehicles to achieve a driving range of 300 miles for early market penetration. The system volumetric capacity target includes a 20% penalty for storage systems that are not conformable to the existing packaging space currently utilized by conventional gasoline tanks. Even more challenging targets have been identified for the 2015 timeframe to enable the required driving range for the full range of light-duty vehicles in the North American market.

*corresponding author

Table 1. Excerpt of U.S. DOE hydrogen storage system performance targets.

Storage Parameter	2010 Target
System Gravimetric Capacity: Usable, specific-energy from H₂ (net useful energy/max system mass)	2 kWh/kg (0.06 kg H₂/kg system or 6 wt.%)
System Volumetric Capacity: Usable energy density from H₂ (net useful energy/max system volume)	1.5 kWh/L (0.045 kg H₂/L system)
Durability/Operability • Operating ambient temperature • Min/max delivery temperature • Cycle life (1/4 tank to full) • Min delivery pressure from tank; FC=fuel cell, ICE=internal combustion engine	−30/50 °C (sun) −40/85 °C 1000 Cycles 4 FC/35 ICE Atm (abs)
Charging/Discharging Rates • System fill time (for 5 kg H₂) • Min full flow rate • Transient response 10%–90% and 90%–0%	3 min 0.02 (g/s)/kW 0.75 s

The DOE storage targets assume a factor of 2.5 to 3 in improved efficiency for the vehicle's fuel cell power plant over today's gasoline ICE vehicle. Assuming the efficiency gains, it is estimated that on-board capacities in the range of 5–13 kg of hydrogen (1 kg hydrogen ~1 gallon of gasoline energy equivalent) would satisfy the needs of the range of today's light-duty fuel cell vehicles.

Much emphasis has been placed on meeting the volumetric and gravimetric targets. While this is central, it must be noted that transient performance must also be achieved by the storage system from "full" tank to "almost depleted." Two key targets noted in Table 1 are the system fill time and the minimum full flow rate. The system fill time, for all methods that involve an exotherm upon hydrogen filling, is strongly dependent upon the thermodynamic properties of the materials (e.g. hydride formation enthalpy or heat of adsorption) and the efficiency of the thermal management system for heat removal and rejection. For example, in order to fill a tank with 8 kg of hydrogen in 5 minutes, a material with a heat of adsorption of 30 kJ/mol will generate heat at a rate of 400 kW. This heat will need to be removed and rejected between the vehicle and the filling station. Conversely, an 80 kW power demand by the fuel cell corresponds to a minimum full flow rate of hydrogen of 1.6 g/s, based on the DOE target of 0.02 g/s/kW. For materials[1] approaches, this hydrogen release rate must be achieved (ideally) at temperatures that can use the waste heat from the PEM fuel cell power plant (e.g. less than 80 °C) over the entire composition range of the material.

In summary, all targets are application driven and not based upon a particular method or technology for storing hydrogen. For commercially acceptable system performance, the targets must be attained simultaneously. For material approaches, it is important to remember that in order to achieve system-level capacities the gravimetric and volumetric capacities of the material alone must clearly be higher than the system-level targets. Recent system developments suggest that, depending on the material and on the system design, material capacities may need to be a factor of up to 2 times higher than system capacity targets.[5]

ALDRICH
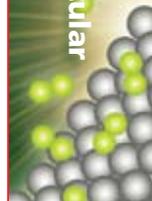
Storage System Technology Status

DOE hydrogen storage research is focused on, but not limited to, materials-based technologies that have the potential to meet DOE's 2010 targets and eventually 2015 targets. Currently, research is focused on achieving the volumetric and gravimetric capacity targets in Table 1, while also meeting the energy and temperature requirements for hydrogen release and the kinetics of hydrogen charging and discharging. In **Figure 1**, the current status of vehicular hydrogen storage systems is shown in comparison to the gravimetric, volumetric and system cost targets. This figure includes R&D data and modeled projections provided by developers, and will be periodically updated by DOE as more data becomes available. The figure also includes a range of tank data from 63 vehicles validated through DOE's "Learning Demonstration" project which includes about 70 hydrogen-fueled vehicles and 10 fueling stations operating to date. Based on operation of these vehicles under "real world" conditions, a driving range of 103 to 190 miles has been achieved thus far (assuming an EPA drive cycle). These vehicles had a hydrogen capacity of about 2 to 4.5 kg. It is evident from Figure 1 that none of the current vehicular hydrogen storage systems meet the combined gravimetric, volumetric, and cost targets for either 2010 or 2015.
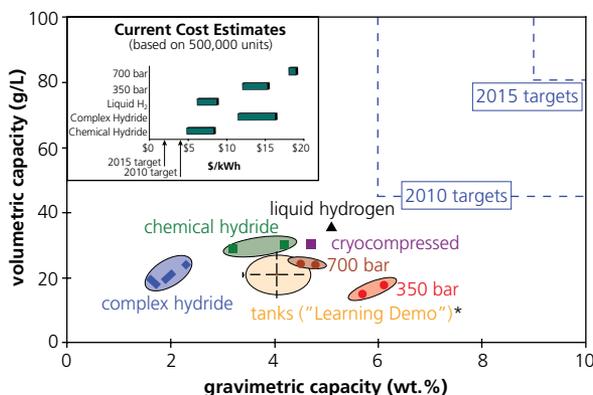
Figure 1. Status of hydrogen storage systems.

Notes on Figure 1: Costs exclude regeneration/processing. Data based on R&D projections and independent analysis (FY05–FY06). To be periodically updated. *Learning Demo data shows range across 63 vehicles.

Research Challenges

On-board hydrogen storage approaches presently being examined by developers include compressed hydrogen gas, cryogenic gas and liquid hydrogen, metal hydrides, high surface area adsorbents, and chemical hydrogen storage media. Compressed and cryogenic hydrogen, adsorbents and some metal hydrides are categorized as "reversible" on-board because these materials may be refilled/recharged with gaseous hydrogen on-board the vehicle, similar to gasoline refueling today. In contrast, chemical hydrogen storage materials generally require a chemical reaction pathway to be regenerated and so the storage system cannot be directly refueled with hydrogen on-board the vehicle. Such systems are referred to as "off-board regenerable," requiring the spent media to be removed from the vehicle and then regenerated with hydrogen either at the fueling station or at a centralized processing facility. Chemical hydrogen storage approaches may also serve as a hydrogen delivery carrier by providing an alternative to transporting hydrogen as a gas or cryogenic liquid.

The various hydrogen storage options under consideration have both common and differing issues. For compressed gas and cryogenic tanks, volume and cost are the primary concerns. Cost and thermal management are issues for all material approaches. For chemical hydrogen storage approaches, the cost and energy efficiency for off-board regeneration are key issues. Research is also needed on improving hydrogen discharge kinetics and simplifying the reactor required for discharging hydrogen on-board the vehicle (e.g. the volume, weight, and operation). For metal hydrides, weight, system volume and refueling time are the primary issues. Volumetric capacity and operating temperature are prime issues for adsorbents that are inherently low density materials and have low hydrogen binding energies thus requiring cryogenic temperature. Finally, for all materials approaches, transient performance and its control for hydrogen discharge is relatively unexplored from a "full" tank to the "nearly depleted" tank.

Summary

The DOE hydrogen storage system targets were developed by translating vehicle performance requirements into storage system needs. The targets are not based upon a particular method or technology for storing hydrogen but for commercially acceptable system performance; they must be attained simultaneously. High pressure or cryogenic hydrogen storage systems are already available in prototype vehicles. DOE-sponsored research is being directed at materials-based approaches with the potential to meet the long-term targets. Details on the DOE's "National Hydrogen Storage Project" and progress made by DOE-funded researchers are available in references 2 through 4. In addition to gravimetric capacity, the R&D community should focus on understanding the volumetric capacity, thermodynamics, kinetics and potential durability/cyclability of materials. Material and system safety is obviously a foremost requirement. The ultimate goal is for storage systems to be integrated with PEM fuel cell power plants, utilizing available waste heat as effectively as possible. Finally, the performance of the storage system must be comparable from a "full tank" to when the owner and vehicle arrive at the filling station with a nearly empty tank. While many promising new approaches have been developed in the last two years, technical challenges remain in order to achieve the 2010 and eventually the 2015 system targets.

References:

(1) http://www.eere.energy.gov/vehiclesandfuels/about/partnerships/freedomcar. The partnership includes the U.S. Council for Automotive Research (USCAR) and the energy companies BP, Chevron, ConocoPhillips, ExxonMobil, and Shell. (2) DOE Office of Energy Efficiency and Renewable Energy Hydrogen, Fuel Cells & Infrastructure Technologies Program Multi-Year Research, Development and Demonstration Plan, available at: http://www.eere.energy.gov/hydrogenandfuelcells/mypp. (3) FY2006 Annual Progress Report for the DOE Hydrogen Program, November 2006, available at: http://www.hydrogen.energy.gov/annual_progress.html.
(4) S. Satyapal et al., FY2006 DOE Hydrogen Program Annual Merit Review and Peer Evaluation Meeting Proceedings, Plenary Session, available at: http://www.hydrogen.energy.gov/annual_review06_plenary.html.
(5) "High Density Hydrogen Storage System Demonstration Using NaAlH₄ Complex Compound Hydrides," Presentation by D. Mosher et al., United Technologies Research Center, prepared under DOE Cooperative Agreement DE-FC36-02AL-67610, December 16, 2006. http://www1.eere.energy.gov/hydrogenandfuelcells/pdfs/storage_system_prototype.pdf

sigma-aldrich.com

TO ORDER: Contact your local Sigma-Aldrich office (see back cover), call 1-800-325-3010 (USA), or visit sigma-aldrich.com/matsci.

Featured Hydrogen Storage Materials and Related Products from Sigma-Aldrich

Featured Hydrogen Storage Materials

IKA® ULTRA-TURRAX® Tube Drive

Personal Workstation for Stirring, Dispersing, and Milling

- Quick and simple to use
- Consistent, reproducible sample prep
- Small foot print
- Economical solution, without risk of cross-contamination

Three tube types enable the IKA® ULTRA-TURRAX® to be used for:

Stirring — Dispersing — Milling

ST-20 Stirring Tube
With built-in stirrer for mixing and stirring volumes 2–15mL
Pack of 25 tubes   Prod. No. **Z722391**

DT-20 Dispersing Tube
With built-in rotor-stator element for dispersion and homogenization of solids and suspensions, volumes 5–15mL
Pack of 25 tubes   Prod. No. **Z722375**

BMT-20G and BMT-20S Ball-Mill Tubes
With glass or stainless-steel balls for dry milling or cell disruption of volumes 2–15mL
Glass beads   Pack of 25 tubes   Prod. No. **Z722413**
SS balls   Pack of 25 tubes   Prod. No. **Z722448**

Order a Workstation Set Now and Receive a Free Swiss Army Knife
(While supplies last)

Workstation set consists of tube drive, power supply, 2 stirring tubes, 2 dispersing tubes and 2 grinding tubes and operating instructions in a compact storage case, ideal for keeping the system neat and tidy when not in use.

Workstation set, with 115V power supply   Prod. No. **Z722332**
Workstation set, with 230V power supply   Prod. No. **Z722456**

IKA is a registered trademark of IKA Works, Inc. Ultra-Turrax is a registered trademark of IKA Works, Inc.

Order: 1.800.325.3010 Technical Service: 1.800.231.8327

ALDRICH®

**For questions, product data, or new product suggestions,
please contact the Materials Science team at matsci@sial.com.**

Recent Developments on Hydrogen Release from Ammonia Borane

Dr. Abhi Karkamkar, Dr. Chris Aardahl, and Dr. Tom Autrey
Pacific Northwest National Laboratory

Introduction

Record crude oil prices combined with public interest in energy security have resulted in increased attention to a potential transportation economy based on hydrogen fuel. One of the greatest challenges is the discovery and development of materials and compounds capable of storing enough hydrogen on-board to enable a 300-mile range without adding significant weight or volume to today's conventional automobile. A minimum of five kilograms of hydrogen would need to be stored on-board to drive even the most fuel-efficient vehicle three hundred miles. At standard temperature and pressure (STP), five kilograms of hydrogen requires a volume of nearly 54 m³. Unfortunately, even highly compressed hydrogen gas is unlikely to be of sufficient volumetric density (40 g/L at 700 bar) to enable a fuel system to meet the 300-mile target. Liquified hydrogen at 70 g/L also falls short of reasonable volumetric system targets when cooling systems required to keep hydrogen liquified (b.p. –253 °C) are added to the storage system.

Many materials with high volumetric and/or gravimetric hydrogen densities have been studied over the last few years, especially those composed of the lighter elements. The driving force for focus on light elements arises from the United States Department of Energy (US DOE) targets for on-board hydrogen storage as outlined in the article by Sunita Satyapal et al. in this issue. It is important to remember that the DOE targets, 60 gm H_2/kg system and 45 gm H_2/L system in 2010 include not just the material, but the entire *storage system*. The storage system is considered as all storage and hydrogen conditioning components leading up to the fuel cell.[1]

Our group and others have been interested in chemical hydrogen storage materials that use the elements nitrogen and boron to chemically bind hydrogen. In these chemical hydrogen storage materials, hydrogen is 'discharged' by a chemical reaction and the hydrogen is 'recharged' by a chemical processing pathway. This makes them unique compared to metal hydride materials or carbon sorbent materials where the hydrogen release and uptake is controlled by temperature and pressure. One compound in particular, ammonia borane (AB = NH_3BH_3) has received significant interest given its stability and commercial availability. Ammonia borane, isoelectronic with ethane, is a solid at room temperature, stable in air and water and contains 190 g/kg (100–140 g/L) hydrogen. **Figure 1** shows that if a large portion of the hydrogen can be liberated, AB has a higher gravimetric density than most other reported chemical systems. This capacity coupled with stability has resulted in renewed interest in studying ammonia borane as a hydrogen storage material. While the material would not be regenerated "on-board" it could potentially meet many DOE targets.

Background on Ammonia Borane

The first published research describing the properties of these AB hydrogen rich materials was funded in large part by U.S. government agencies interested in boron-based jet fuels.[2] Ammonia borane was first synthesized and characterized by Sheldon Shore in the 1950s during his thesis research in Richard Parry's lab at the University of Michigan.[3] They performed a series of clever experiments designed to identify the 'mysterious' $B_2N_2H_6$ adduct, the so-called diammoniate of diborane (DADB), formed when ammonia was mixed with diborane. The same adduct appeared to be formed when an ammonium salt was mixed with a metal borohydride in liquid ammonia. Previous work had suggested that the reaction produced an ammonium cation and the corresponding diborane anion $[NH_2(BH_3)_2][NH_4]$. However, there was no unambiguous evidence to rule out the formation of the isomeric borohydride salt $[BH_2(NH_3)_2][BH_4]$.[3,4]

One of the key experiments used to elucidate the true structure of DADB was to add an ammonium salt (NH_4Cl) to DADB. If the structure of DADB was $[NH_4][BH_3NH_2BH_3]$ then no change in reactants would be observed, however, if DADB

Figure 1. Comparison of gravimetric and volumetric densities of various hydrogen storage materials.

were the alternate isomer consisting of a borohydride anion, $[BH_2(NH_3)_2][BH_4]$, then an exchange reaction would occur to yield $[BH_2(NH_3)_2]Cl + NH_4BH_4$. When Shore and Parry performed the reaction they did see the predicted chloride salt, but they also observed a new material that proved to be NH_3BH_3 (Eq. 1).[3]

$$[BH_2(NH_3)_2][BH_4] + NH_4Cl \xrightarrow[\text{Small amt of NH}_3]{\text{diethyl ether}} [BH_2(NH_3)_2]Cl + NH_3BH_3 + H_2 \quad (1)$$
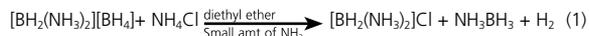
Subsequent work showed that NH_4BH_4 was unstable and decomposed to ammonia borane and hydrogen with a half life of hours at room temperature.[5]

Alternate pathways have been developed to simplify the synthesis and increase the yield of ammonia borane. NH_3BH_3 can be prepared by a reaction of alkali metal borohydride and ammonium chloride in diethyl ether at room temperature. (Eq. 2) Similar reactions are used to synthesize alkylaminoboranes such as $(CH_3)_3NBH_3$. Additionally NH_3BH_3 can be prepared by a reaction of diethyl ether-borane with ammonia in yields of up to 70% (Eq. 3).

$$NaBH_4 + NH_4Cl \xrightarrow{\text{diethyl ether}} NH_3BH_3 + NaCl + H_2 \quad (2)$$

$$H_3B \cdot OEt_2 + NH_3 \xrightarrow{\text{diethyl ether}}_{\text{-78 °C}} NH_3BH_3 \quad (3)$$
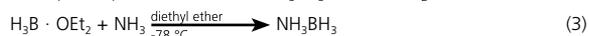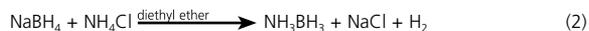
A simple molecular description of NH_3BH_3 shows that it is a donor-acceptor adduct formed as a result of the dative bond between a Lewis acid (BH_3) and a Lewis base (NH_3). The compound is a solid at room temperature primarily due to di-hydrogen bonding and dipole-dipole interactions.[6] Though ammonia borane and diammoniate of diborane have the same chemical formula they are very different in stability. Ammonia borane is soluble in ether while the diammoniate of diborane is not. Ammonia borane is not readily hydrolyzed by water while diammoniate of diborane reacts instantaneously with water. Over time solid DADB slowly converts to solid AB at room temperature. Thus AB is more readily applicable than DADB to hydrogen storage for automotive use.

Hydrogen Release Studies

Recent work has shown that NH_3BH_3 can release more than 2 moles of H_2 with heating to modest temperature. The reactions of hydrogen evolution can be summarized as shown in equations 4 through 7.

$$nNH_3BH_3 \xrightarrow{\Delta} (NH_2BH_2)_n + (n-1)H_2 \ (<120 °C) \ \text{(intermolecular)} \quad (4)$$

$$(NH_2BH_2)_n \xrightarrow{\Delta} (NHBH)_n + H_2 \ (\sim150 °C) \ \text{(intramolecular)} \quad (5)$$

$$2(NHBH)_n \xrightarrow{\Delta} (NHB{-}NBH)_x + H_2 \ (\sim150 °C) \ \text{(cross linking)} \quad (6)$$

$$(NHBH)_n \xrightarrow{\Delta} BN + H_2 \ (> 500 °C) \ \text{(boron nitride)} \quad (7)$$
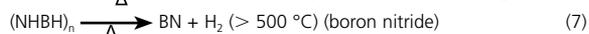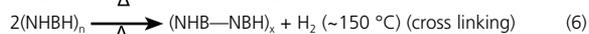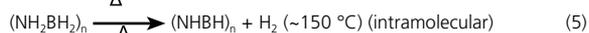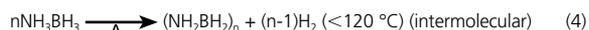
The first two steps, reaction of AB to form PAB, polyaminoborane, $(NH_2BH_2)_n$; and PAB to form PIB, polyiminoborane $(NHBH)_n$ amount to 12 mass% hydrogen. The hydrogen release in these first two steps occurs at temperatures less than 150 °C. At a slightly higher temperature the cross-linking between molecules is observed to release additional hydrogen. These materials are common intermediates used as precursors to boron nitride, which is formed at temperatures much greater than 500 °C.[7–10]

Efficient methods are needed to dehydrogenate ammonia borane to release hydrogen at moderate temperatures and reasonable rates. Various groups have used different methods to study and catalyze the dehydrogenation reaction. Here we review five different approaches used to release hydrogen from ammonia borane.

1. Solid state thermal decomposition
2. Transition metal catalyzed dehydrogenation
3. Ionic liquid catalyzed dehydrogenation
4. Solution phase thermal decomposition
5. Nanophase ammonia borane encapsulated in SBA-15

Solid State Thermal Decomposition

Geanangel was one of the first researchers to report studies on the thermal dissociation of AB using thermomanometry, pyrolysis, DSC, DTA and TGA in the early to late 1980s.[11–13] The DTA curves showed a sharp endothermic peak beginning at just above 112 °C, which corresponds to the melting point of pure AB (112–114 °C). On further heating thermomanometry showed a sharp pressure rise near 120 °C due to hydrogen evolution. That corresponded to the first exothermic peak in the DTA at 117 °C, which accompanies vigorous decomposition as can be seen by the mass loss in the TGA data. Upon further heating the rate of pressure increase slowed as the hydrogen evolution from the first step reached completion. Continued temperature increase resulted in the release of a second equivalent of H_2.

In more recent studies, Wolf and co-workers in Freiberg, Germany have revisited the thermal analysis of AB using controlled calorimetric studies to identify the events leading to dehydrogenation and isolation of products obtained in the process. They also explored the effect of experimental conditions such as heating rate and pressure on the thermal decomposition of AB.[7–9] As expected even high overpressure of hydrogen neither significantly impacted the hydrogen release rate nor the enthalpic parameters during the thermal decomposition since both the transitions (AB $\longrightarrow$ PAB and PAB $\longrightarrow$ PIB) are exothermic. Furthermore, there was little change in the quantities of volatile products generated. On the other hand, they report that the rate of heating appears to have a measurable impact on the thermal events and the volatile product formation. Higher heating rates resulted in greater quantities of volatile products such as borazine.[7–9] The formation of volatile products in the absence of subsequent hydrogen purification will be problematic for PEM fuel cells that are easily fouled by contaminants in the hydrogen stream.

Transition Metal Catalyzed Dehydrogenation of Ammonia Borane in Solution

Chandra et al. reported the transition metal catalyzed dehydrogenation of AB under aqueous conditions and suggest that the activation process takes place on the metal catalyst surface.[14,15] As a plausible mechanism, it is reasonable to consider that there should be interactions between the NH_3BH_3 molecule and the metal particle surface to form an activated complex which upon attack by a H_2O molecule readily leads to a concerted dissociation of the B–N bond and hydrolysis of the resulting BH_3 byproduct to produce the boric acid and H_2. Interestingly, in the absence of H_2O, dehydrocoupling between NH_3BH_3 molecules to form new B–N bonds occurs, probably via a closely related intermediate, on the metal surface. In their studies Pt supported on carbon was the most efficient catalyst for dehydrogenation. Alternatively Denney and Goldberg[16]

reported use of molecular complexes of transition metals (e.g. Ir) containing pincer ligands for dehydrogenation at room temperature in just 14 minutes, considerably faster than the previously reported rhodium complexes (dehydrogenation of dimethyl amino borane required 2–4 days at 45 °C).[17] The plausible reason for this difference in rates is homogeneous vs. heterogeneous catalysis wherein the Ir complex catalyzes the dehydrogenation by a homogeneous pathway while the rhodium catalyst undergoes a transformation to a rhodium colloid or cluster. It is interesting to note that most of the product obtained as a result of dehydrogenation is a pentamer having the formula $(BH_2NH_2)_5$ (Eq. 8).

$$n\ NH_3BH_3 \xrightleftharpoons{[catalyst]} [H_2NBH_2]_n + n\ H_2 \qquad (8)$$
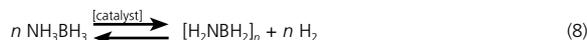
Here the catalysis is performed by $(POCOP)Ir(H)_2$; (POCOP) is $[\eta^3\text{-}1,3\text{-}(OP t Bu_2)_2C_6H_3])$.

Linehan[17] reported that a Rh catalyst has been shown to release one third of the available H_2 from dimethylamino borane $((CH_3)_2NHBH_3)$ under ambient conditions. It is thus important to not only determine the active form of the catalyst for this reaction but to also understand, in detail, the reaction pathway and kinetics for the amine borane dehydrocoupling. Earlier studies proposed that Rh nanoparticles were the catalytic species as determined from ex situ measurements of the Rh species. X-ray absorption fine structure (XAFS) and NMR demonstrated that nanoparticles are not present during this reaction but rather, small Rh_n clusters (n=4–6) are the predominant species during dehydrocoupling. Such in situ techniques probe the catalyst not only in the reaction solvent and at the reaction pressure and temperature, but also while it is undergoing chemical reactions with the reactants in the system. In situ XAFS and NMR are especially useful for following the reaction pathways and kinetics of the reactants, the products and for catalyst characterization (**Figure 2**).
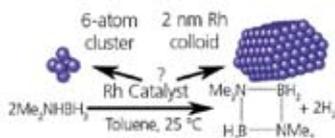
Figure 2. Schematic pathway of formation of Rh clusters during the dehydrogenation of dimethylamino-borane (DMAB). Reprinted with permission from Ref. 17 ©2006 American Chemical Society.

Dehydrogenation of Ammonia Borane in Ionic Liquids

Ionic liquids are salts that are liquid at temperatures below 100 °C. These salts have unique properties that make them attractive substitutes for organic solvents in hydrogen storage systems, including: (1) negligible vapor pressures; (2) stable to elevated temperatures; (3) able to dissolve a wide range of compounds and gases; (4) weakly coordinating anions and cations that provide an inert reaction medium which can stabilize polar transition states; and (5) recyclable with little loss of activity.

Bluhm and Sneddon recently reported dehydrogenation of AB in ionic liquids such as 1-butyl-3-methylimidazolium chloride [bmimCl] and compared it to solid-state dehydrogenation.[18] In contrast to the solid-state reaction, ammonia borane dehydrogenation in bmimCl showed no induction period with hydrogen evolution beginning immediately upon placing the sample in the heated oil bath. Separate samples heated for only 1 h at 85, 90, and 95 °C evolved 0.5, 0.8, and

1.1 equiv of H_2, while samples heated at these temperatures for 3 h produced 0.95, 1.2, and 1.5 equiv. Heating for 22 h gave a total of 1.2, 1.4, and 1.6 equiv of H_2, respectively, which are values significantly greater than the 0.9 equiv ultimately obtained in the solid-state reactions. Including the bmimCl weight, the final values correspond to the evolution of 3.9, 4.5, and 5.4 wt % H_2. The role of bmimCl in enhancing the rate and extent of ammonia borane dehydrogenation has yet to be proven, but it is significant that $[(NH_3)_2BH_2^+]BH_4^-$ has also been reported to form polyaminoborane upon heating. (**Figure 3**) Ionic liquids are known to favor the formation of polar intermediates and transition states, and the observation that $[(NH_3)_2BH_2^+]BH_4^-$ and/or BH_4^- are produced in the bmimCl reaction within the first hour suggests that the activating effect of the ionic liquid may be related to its ability to induce formation of such ionic species.
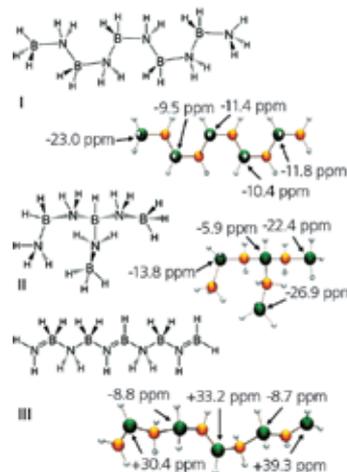
Figure 3. The possible structures arising from dehydropolymerization of AB using DFT/GIAO calculated values of ^{11}B NMR. Reprinted with permission from Ref. 18 ©2006 American Chemical Society.

Solution Phase Thermal Dehydrogenation

The thermal decomposition of ammonia-borane in selected solvents was studied by Geanangel using ^{11}B NMR at temperatures up to and including reflux in various solvents. Solvents chosen dissolved NH_3BH_3 to a reasonable concentration and possess boiling temperatures of 80 °C, the lowest temperature at which ammonia-borane decomposes at an acceptable rate.[19] Solvents such as alcohols, which undergo solvolytic reactions with ammonia-borane, were not included in the study. The purpose of the work was to identify solvents and conditions best suited for preparing and carrying out reactions of NH_2BH_2 generated thermally from ammonia borane. It was hoped that NH_2BH_2, which is subject to facile association in the solid phase, would be stabilized sufficiently by solvation to be at least detectable in solution. If not, the quantities of its oligomers detected in the reaction mixtures would indicate the extent of its formation. Three types of reactions were observed: (1) hydrogen-loss decomposition of NH_3BH_3 leading to cycloborazane(s) and eventually to borazine, (2) base displacement by solvent on NH_3BH_3 giving a solvent-borane adduct, and (3) reaction with the solvent leading to products consistent with a hydroboration pathway. The etheral solvents glyme, diglyme, tetrahydrofuran and 2-methyltetrahydrofuran gave mainly products suggesting hydrogen-loss decomposition of NH_3BH_3.

TO ORDER: Contact your local Sigma-Aldrich office (see back cover), call 1-800-325-3010 (USA), or visit sigma-aldrich.com/matsci.

ALDRICH

sigma-aldrich.com

Nanophase Ammonia Borane in Mesoporous SBA-15

Gutowska reported the preparation of nanophase AB by incorporating AB into the channels of mesoporous silica SBA-15 (**Figure 4**).[20] This resulted in significantly different behavior lowering the dehydrogenation temperature from 114 °C to 85 °C accompanied by a relatively low exothermicity. The two other notable effects resulting from the nanostructure of AB in the SBA-15 scaffold include: 1) the temperature threshold for H_2 release (m/e=2) being notably lower than the temperature threshold for neat AB indicative of an enhanced rate of H_2 release; and 2) the yield of the borazine side product (m/e=80) is significantly lower than for neat AB. **Figure 5** shows the effect of mesoporous silica encapsulation on thermodynamics of ammonia borane. Solid-state ^{11}B NMR spectroscopy was used to analyze the nonvolatile products from neat AB and AB:SBA-15 to see if the borazine became entrapped within the mesoporous scaffold. However, no [11]B signal for borazine was observed. Because borazine is not observed as a volatile product in the TPD/MS experiment, and not detected by solid-state NMR spectroscopy, the mesoporous scaffold appears to affect the decomposition pathways of AB that lead to hydrogen formation.
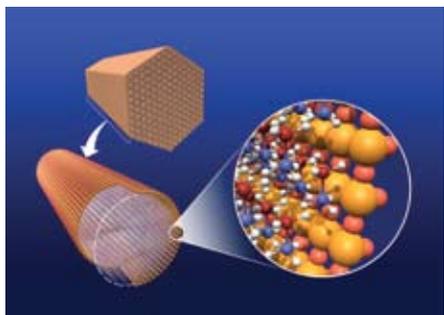
Figure 4. Illustration depicting incorporation of ammonia-borane into the channels of mesoporous silica SBA-15.
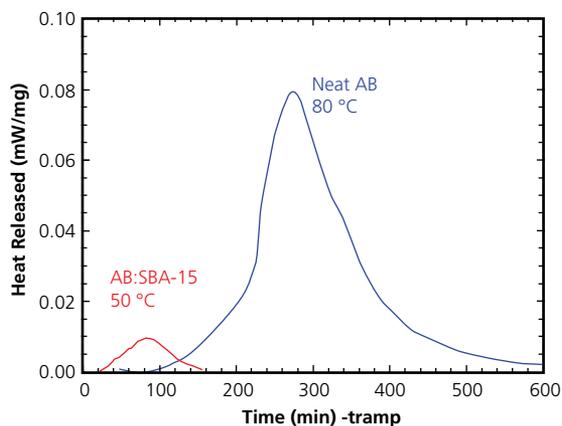
Figure 5. Isothermal DSC comparisons showing lower reaction enthalpy for H_2 loss from AB on mesoporous silica SBA-15.

Summary

While ammonia borane looks promising for hydrogen storage, given the volumetric and gravimetric density of hydrogen in the material, there are still technical challenges to be addressed. Foremost of these challenges are (1) enhancing the rates of hydrogen release and (2) the discovery of economical chemical processing pathways that will be used to put the hydrogen back on to the dehydrogenated materials. Our group is currently focusing on these technical challenges.

References:

(1) Satyapal, S.; Petrovic, J.; Read, C.; Thomas, G.; Ordaz, G. *Catal. Today* **2007**, *120*, 246. (2) Schubert, D., M. *Borax Pioneer* **2001**, *20*. (3) Shore, S. G.; Parry, R. W. *J. Am. Chem. Soc.* **1955**, *77*, 6084. (4) Shore, S. G.; Parry, R. W. *J. Am. Chem. Soc.* **1958**, *80*, 8. (5) Parry, R. W.; Schultz, D. R.; Girardot, P. R. *J. Am. Chem. Soc.* **1958**, *80*, 1. (6) Weaver, J. R.; Shore, S. G.; Parry, R. W. *J. Chem. Phys.* **1958**, *29*, 1. (7) Baitalow, F.; Baumann, J.; Wolf, G.; Jaenicke-Rossler, K.; Leitner, G. *Thermochim. Acta* **2002**, *391*, 159. (8) Wolf, G.; Baumann, J.; Baitalow, F.; Hoffmann, F. P. *Thermochim. Acta* **2000**, *343*, 19. (9) Wolf, G.; van Miltenburg, J. C.; Wolf, U. *Thermochim. Acta* **1998**, *317*, 111. (10) Baumann, J.; Baitalow, F.; Wolf, G. *Thermochim. Acta* **2005**, *430*, 9. (11) Sit, V.; Geanangel, R. A.; Wendlandt, W. W. *Thermochim. Acta* **1987**, *113*, 379. (12) Komm, R.; Geanangel, R. A.; Liepins, R. *Inorg. Chem.* **1983**, *22*, 1684. (13) Hu, M. G.; Geanangel, R. A.; Wendlandt, W. W. *Thermochim. Acta* **1978**, *23*, 249. (14) Xu, Q.; Chandra, M. *J. Power Sources* **2006**, *163*, 364. (15) Chandra, M.; Xu, Q. *J. Power Sources* **2006**, *156*, 190. (16) Denney, M. C.; Pons, V.; Hebden, T. J.; Heinekey, D. M.; Goldberg, K. I. *J. Am. Chem. Soc.* **2006**, *128*, 12048. (17) Chen, Y. S.; Fulton, J. L.; Linehan, J. C.; Autrey, T. *J. Am. Chem. Soc.* **2005**, *127*, 3254. (18) Bluhm, M. E.; Bradley, M. G.; Butterick, R., III; Kusari, U.; Sneddon, L. G. *J. Am. Chem. Soc.* **2006**, *128*, 7748. (19) Wang, J. S.; Geanangel, R. A. *Inorg. Chim. Acta* **1988**, *148*, 185. (20) Gutowska, A.; Li, L. Y.; Shin, Y. S.; Wang, C. M. M.; Li, X. H. S.; Linehan, J. C.; Smith, R. S.; Kay, B. D.; Schmid, B.; Shaw, W.; Gutowski, M.; Autrey, T. *Angew. Chem. Int. Ed.* **2005**, *44*, 3578.

Dehydrogenation of Ammonia Borane

Order: 1.800.325.3010 Technical Service: 1.800.231.8327

ALDRICH®

Ammonia Borane-Based Hydrogen Storage—Dehydrogenation Media and Catalysts

Dehydrogenation of Ammonia Borane

Name	Structure	Purity (%)	Prod. No.
Borane ammonia complex	$H_3N–BH_3$	>90	**287717-1G** **287717-10G**
Dehydrogenation Catalysts/Catalytic Systems			
Bis(1,5-cyclooctadiene)dirhodium(I) dichloride		98	**227951-500MG** **227951-5G**
Bis(1,5-cyclooctadiene)diiridium(I) dichloride		97	**275131-100MG** **275131-500MG**
Bis(1,5-cyclooctadiene)nickel(0)		20.0–22.6% Ni content	**244988-2G**
N-Heterocyclic Carbene Ligands Kit I	A set of 5 ligand precursors for Ni catalysts; components are listed below		**662232-1KT**
Ionic Liquids*			
1,3-Bis-(2,6-diisopropylphenyl)imidazolinium chloride**		97	**656623-1G** **656623-5G**
1,3-Bis-(2,4,6-trimethylphenyl)imidazolinium chloride**		95	**656631-1G** **656631-5G**
1,3-Diisopropylimidazolium tetrafluoroborate**		96	**660019-1G** **660019-5G**
1,3-Bis(1-adamantyl)imidazolium tetrafluoroborate**		97	**660035-1G**
1,3-Di-*tert*-butylimidazolinium tetrafluoroborate**		95	**659991-1G** **659991-5G**
1-Butyl-3-methylimidazolium chloride		99	**04129-5G-F** **04129-25G-F**
1-Butyl-3-methylimidazolium bromide		>98.5	**64133-5G** **64133-25G**
1-Butyl-3-methylimidazolium hydrogen carbonate		>97	**670723-10G** **670723-100G**
1-Butyl-3-methylimidazolium tetrafluoroborate		>97	**91508-5G** **91508-50G** **91508-250G**
1-Butyl-3-methylimidazolium hexafluorophosphate		>96	**70956-5G** **70956-50G** **70956-250G**
1-Butyl-3-methylimidazolium dibutyl phosphate		>96	**669733-5G** **669733-50G**
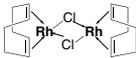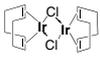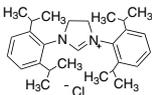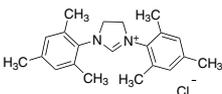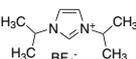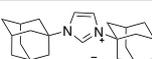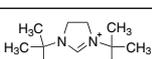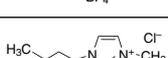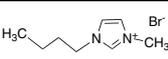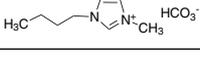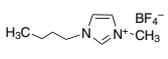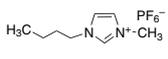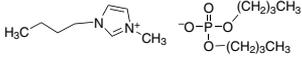
*For more ionic liquids see *ChemFiles*™ 2005, Vol. 5, No. 6. and visit **sigma-aldrich.com**.
**Components of the Carbene Ligands Kit I.

Metal Borohydrides as Hydrogen Storage Materials

Dr. Grigorii L. Soloveichik
General Electric Global Research

Introduction

To meet current DOE targets outlined in the article by S. Satyapal et al. in this issue, the materials for hydrogen storage should possess high hydrogen content, low heats of dehydrogenation (to minimize the energy penalty), and fast kinetics of hydrogen desorption at operation temperatures of a PEM fuel cell (80–120 °C). Of the number of different options being considered, solid metal hydrides that reversibly desorb large amounts of hydrogen are extremely attractive as base materials for hydrogen storage due to process simplicity, low operation pressures, and relatively low cost.

Early work in the area of hydrogen storage concentrated on intermetallic hydrides like $LaNi_5$ and TiFe, which showed very good sorption/desorption kinetics but had low hydrogen storage capacities (below 2% of hydrogen by weight). Numerous attempts to increase their capacity and keep good kinetics by making polymetallic compositions with lightweight metals were unsuccessful.

A subsequent wave of research interest was aimed at sodium aluminum hydride (or alumohydride, or alanate), $NaAlH_4$, after Bogdanovič found that titanium catalysts decrease the desorption temperature of $NaAlH_4$ and make this process reversible.[1] This work showed that complex metal hydrides might be used as reversible hydrogen storage materials. However, relatively low capacities of complex metal alumohydrides, except $LiAlH_4$ (10.5%), and complexity of their decomposition constitute a serious problem to be resolved before their commercialization. Aluminum hydride AlH_3, which contains 10 wt. % of hydrogen, smoothly decomposes in one step at moderate temperature but can be regenerated only at very high pressure (24 Kbar).[2]

Complex metal borohydrides $M(BH_4)_n$ with their high hydrogen content (**Table 1**) and the potential to meet DOE targets are of growing interest. Their synthesis and properties related to hydrogen storage are briefly discussed below.

General Synthetic Methods

The first metal borohydride, $LiBH_4$, was synthesized by Schlesinger and Brown more than 65 years ago using the reaction of ethyllithium with diborane.[18] Although discovered at about the same time, the synthesis of sodium borohydride, $NaBH_4$, was reported much later.[19] $NaBH_4$ is the most widely commercially produced borohydride and is used in the paper and textile industries, and as a reducing agent in organic synthesis.[20] It is also a commonly used starting material for synthesis of other metal borohydrides.

The direct synthesis from the elements at elevated pressure and temperature was claimed for borohydrides of Li, Na, K, Mg, and Ba.[21] In practice only indirect methods are used for synthesis of metal borohydrides.

Four general methods are used for the preparation of metal borohydrides: i) addition of diborane, B_2H_6, to metal hydrides, ii) reaction of B_2H_6 with metal alkyls or metal alkoxides, iii) reaction of metal hydrides with boron compounds, and iv) exchange reaction between metal borohydrides and other metals salts, mostly halides. Historically, reactions based on the use of diborane were employed first. If the metal hydride

Table 1. Properties of metal borohydrides.

Hydrogenated form	Dehydrogenated form	Hydrogen capacity wt. %	g H₂/L	−ΔH, kJ/mol H₂	Decomp. temp., °C calc.	obs.	Reference
$LiBH_4$	LiH + B	13.9	93	75	402	470	3,4
$2\ LiBH_4 + MgH_2$	$3\ LiH + MgB_2$	11.4		46	225	315	5,6
$2\ LiBH_4 + Al$	$2\ LiH + AlB_2$	8.6			188		6
$7\ LiBH_4 + 1.75\ Mg_2Sn + 0.25\ Sn$	$Li_7Sn_2 + 3.5\ MgB_2$	6.3		46	184		4
$NaBH_4$	NaH + B	7.9	85.5	90	609	595	3,4
$2\ NaBH_4 + MgH_2$	$3\ NaH + MgB_2$	7.8		62	351		4,7
$Be(BH_4)_2$	Be + 2B	20.8	126	27		123	8
$Mg(BH_4)_2$	Mg + 2B	14.9	113	40		323	3,8,9
$Ca(BH_4)_2$	$2/3\ CaH_2 + 1/3 CaB_6$	9.7	108	75.5		360	10,11
$Ca(BH_4)_2 + MgH_2$	$CaH_2 + MgB_2$	8.3			159		4
$Zn(BH_4)_2$	Zn + 2B*	8.5				85	12
$Al(BH_4)_3$	Al + 3B*	16.9	121	6		150	13,14
$Sc(BH_4)_3$	ScB_2 +B (?)	13.5				260	15
$Ti(BH_4)_3$	TiB_2 +B*	13.1				25	16
$Mn(BH_4)_2$	Mn + 2B	9.5					–
$Zr(BH_4)_4$	ZrB_2 + 2B (?)	10.7	108			250	17

*Formation of diborane observed.

is stable, such as hydrides of Li, Na, and Mg, reaction (Eq. 1) proceeds smoothly to the metal borohydride. However, if the metal hydride is unstable, like hydrides of Be and Al, a metal alkyl or alkoxide should be used (Eq. 2).

$$MH_n + n/2\ B_2H_6 \longrightarrow M(BH_4)_n \tag{1}$$

$$Al_2Me_6 + 4\ B_2H_6 \longrightarrow 2\ Al(BH_4)_3 + 2\ BMe_3 \tag{2}$$
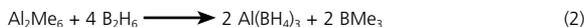
In the case of alkali earth metal borohydrides (M = Mg, Ca, Sr, Ba) alkyldiboranes are used instead of B_2H_6, the reactions are carried out without solvent (Eq. 3), and boralkyls are removed by distillation to give pure products.[22]

$$MH_2 + 3\ B_2H_2Pr_4 \longrightarrow M(BH_4)_2 + 4\ BPr_3 \tag{3}$$
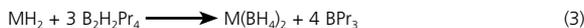
The toxicity, high flammability, and low thermal stability of diborane make processes based on Eqs. 1 and 2 impractical. Instead, processes using in situ generation of diborane have been developed. Under the right conditions, reaction of metal hydrides (Eq. 4) or alumohydrides (Eq. 5) with BF_3 etherate or alkylborates leads to the preparation of metal borohydrides via intermediate B_2H_6.

$$4\ LiH + BF_3{\cdot}Et_2O \longrightarrow LiBH_4 + 3\ LiF{\downarrow} + Et_2O \tag{4}$$

$$LiAlH_4 + B(OMe)_3 \longrightarrow LiBH_4 + Al(OMe)_3 \tag{5}$$

The exchange reaction (Eq. 6) is a common method for the preparation of binary metal borohydrides $M(BH_4)_n$ as well as multiple metal borohydride complexes stabilized by donor ligands.

$$MX_n + n\ M'BH_4 \longrightarrow M(BH_4)_n + n\ M'X \tag{6}$$
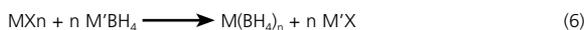
Li or Na borohydrides are usually used as a source of BH_4-group but borohydrides of other metals (K, Ca, Al) can also be used. This reaction usually takes place in donor solvents (ethers, amines), where one or both reagents are soluble but one of the reaction products, usually an alkali metal chloride, is not. Metal borohydrides are isolated from solution as solvates with one or more molecules of the solvent. Therefore, this process requires an additional desolvation step. However, thermal desolvation, often in vacuum, in some cases can lead to the decomposition of $M(BH_4)_n$ with H_2 evolution preceding the desolvation point. In such cases, unsolvated borohydrides can be prepared by mechanochemical exchange reactions (e.g. using ballmilling); see also the article by V. Balema in this issue. This method is very convenient for volatile borohydrides, such as those of Be, Al, and Zr, which can be isolated by distillation or sublimation.[23] However, for nonvolatile $M(BH_4)_n$ the removal of the M'X byproduct is very difficult.

Synthesis and Properties of Some Metal Borohydrides

Lithium borohydride LiBH₄ (Aldrich Prod. No. **222356**) has been prepared using all of the previously described synthetic methods. Probably, the most practical one is the exchange reaction of LiCl with NaBH₄ in isopropylamine.

$LiBH_4$ is a white solid with density of 0.68 g/cm^3. It exists in two crystal modifications (orthorhombic transforms to tetragonal at 108 °C) and melts at 278 °C. It reacts violently with water to produce H_2 but relatively stable in dry air.

Decomposition of liquid $LiBH_4$ with hydrogen evolution starts at 320–380 °C (470 °C under 10 atm H_2 pressure)[3]. In earlier work it had been reported that during the decomposition only 50% of hydrogen was released and an unidentified phase "$LiBH_2$" formed.[18] In later work it was reported that the $LiBH_4$ decomposition liberates ~80% of total hydrogen at ambient pressure[24] and 75% at 10 atm H_2[3] (Eq. 7). However, in the most recent publication[25] the formation of "$LiBH_2$" and perhaps other intermediates (at low heating rates) has been confirmed.

$$LiBH_4 \longrightarrow LiH + B + 3/2\ H_2 \tag{7}$$

Sodium borohydride NaBH₄ (Aldrich Prod. Nos. **480886**; **452882**; **452874**; **452173**; **452165**) is a high melting (505 °C) solid with relatively low reactivity. Its basic solution in water is stable to hydrolysis.

Two processes for $NaBH_4$ manufacturing have been commercialized. Probably the most convenient is the borate method, developed in the U.S., where methylborate reacts with sodium hydride in mineral oil (Eq. 8). This reaction does not require hydrogen pressure but occurs at 250–280 °C, temperatures necessary to melt and disproportionate the intermediate $Na[HB(OCH_3)_3]$. Dissolution of the reaction mixture in water and extraction with isopropylamine gives the dihydrate that can be desolvated by heating in vacuum to give pure $NaBH_4$.

$$4\ NaH + B(OCH_3)_3 \longrightarrow NaBH_4 + 3\ NaOCH_3 \tag{8}$$
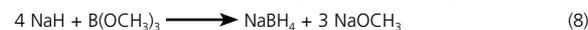
The borosilicate process developed by Bayer (Eq. 9) uses less expensive boron compounds but requires higher temperature (400–500 °C) and hydrogen pressure. Isolation of $NaBH_4$ involves extraction with liquid NH_3 under pressure.

$$(Na_2B_4O_7 + 7\ SiO_2) + 16\ Na + 8\ H_2 \longrightarrow 4\ NaBH_4 + 7\ Na_2SiO_3 \tag{9}$$

Because of the potential use of $NaBH_4$ for hydrogen generation by catalytic hydrolysis, its regeneration from the borate $NaBO_2$ is being studied intensively. An analysis of the thermodynamics of more than 30 reactions leading to $NaBH_4$ showed that the use of calcium hydride (Eq. 10) for this purpose is the most favorable approach.[26]

$$NaBO_2 + 2\ CaH_2 \longrightarrow NaBH_4 + 2\ CaO \tag{10}$$
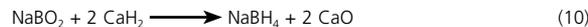
Beryllium borohydride Be(BH₄)₂ has the highest total hydrogen capacity (Table 1). It was originally prepared by reaction of $BeMe_2$ with diborane[27] and, more conveniently, by mechanochemical exchange reaction of $BeCl_2$ with alkali metal borohydrides followed by vacuum distillation at 140 °C.[28] This covalent compound is built of helical polymeric chains $-BeH_2BH_2BeH_2BH_2-$ and terminal bidentate BH_4-groups.[29] The covalent character of Be–BH_4 bonding explains the high volatility of $Be(BH_4)_2$ and, therefore, also its extremely high reactivity (it explodes on contact with air and moisture). Unfortunately, the extreme toxicity of beryllium, and very high reactivity of $Be(BH_4)_2$, makes this material unsuitable for hydrogen storage despite low decomposition temperature and ΔH_f.

TO ORDER: Contact your local Sigma-Aldrich office (see back cover), call 1-800-325-3010 (USA), or visit sigma-aldrich.com/matsci.

sigma-aldrich.com

ALDRICH®

Magnesium borohydride Mg(BH₄)₂ was first reported more than 50 years ago.[30] Plešek and Heřmánek isolated the unsolvated magnesium borohydride using reaction of MgH_2 with diborane (Eq. 1).[31] Konoplev and Bakulina reported the synthesis of unsolvated $Mg(BH_4)_2$ by exchange reaction (Eq. 6) of $MgCl_2$ with $NaBH_4$ and provided the X-ray diffraction (XRD) pattern of its two crystal modifications.[32] Literature data on solvent-free $Mg(BH_4)_2$ synthesis and properties are contradictory as well as attempts to predict its structure. Our group at GE GRC prepared two crystal modifications of $Mg(BH_4)_2$ with an XRD pattern different from the reported in Ref. 32 using a modified exchange method. A hexagonal phase, which is stable at room temperature, converts to an orthorhombic phase at 185 °C, which also can be stored at room temperature.[33] Both phases have complex networks of corner-sharing tetrahedra consisting of a central Mg atom and four BH_4 units. Differential scanning calorimetry (DSC) of $Mg(BH_4)_2$ shows two endothermic peaks at 300 and 376 °C, and one exothermic peak at 357 °C that can be assigned to decomposition of $Mg(BH_4)_2$, crystallization of amorphous MgH_2, and decomposition of MgH_2 into elements (Eq. 11).[33] Structures of both phases of $Mg(BH_4)_2$ and their properties will be published elsewhere.

$$Mg(BH_4)_2 \longrightarrow 3\,H_2 + 2\,B + MgH_{2\,(amorph)} \longrightarrow MgH_{2\,(cryst)} \longrightarrow Mg + H_2 \quad (11)$$

Calcium borohydride Ca(BH₄)₂ (Aldrich Prod. No. **389986**; **21057**) has been prepared by the reaction of diborane with calcium hydride[34] or alkoxides[35] but an exchange reaction between $CaCl_2$ and $NaBH_4$ in a ball mill[10] or in THF[36] are more convenient ways of making it. Desolvation of the $Ca(BH_4)_2 \cdot 2THF$ adduct occurs easily in vacuum at 190 °C.[36] $Ca(BH_4)_2$ is a non-volatile solid with density 1.12 g/cm³. It is completely stable in dry air and soluble in water without decomposition.

Unsolvated $Ca(BH_4)_2$ has an ionic structure with Ca^{2+} ions surrounded by six tetrahedral BH_4-groups and each BH_4-group contacts with three Ca^{2+} ions.[11] Despite relatively low hydrogen capacity, the volumetric hydrogen density of $Ca(BH_4)_2$ is comparable with that of $Mg(BH_4)_2$ due to its higher density (Table 1). Decomposition of $Ca(BH_4)_2$ begins at 360 °C but is complete only at 500 °C and releases 9.6% hydrogen according to Eq. 12, which was predicted on the basis of the calculated heat of formation.[11]

$$Ca(BH_4)_2 \longrightarrow 2/3\,CaH_2 + 1/3\,CaB_6 + 10/3\,H_2 \quad (12)$$

Zinc borohydride Zn(BH₄)₂ in a solvent-free form was made by ball-milling of $ZnCl_2$ and $NaBH_4$ as a mixture with NaCl.[12] According to DSC data, unsolvated $Zn(BH_4)_2$ melts at about 95 °C with decomposition.[12] The decomposition is endothermic and proceeds with the formation of diborane (Eq. 13).[12]

$$Zn(BH_4)_2 \longrightarrow Zn + B_2H_6 + H_2 \quad (13)$$

Aluminum borohydride Al(BH₄)₃ was first prepared by reaction of trimethylaluminum with diborane,[18] but the mechanochemical exchange reaction of $AlCl_3$ and $NaBH_4$ followed by vacuum distillation of the target product into cooled traps is much more practical.[37] $Al(BH_4)_3$ is a liquid (m.p. –64 °C) and its structure was determined by low temperature single crystal X-ray diffraction.[38] Both modifications (phase transformation temperature is about 180 K) are built of discrete molecular units with similar geometry: the aluminum atom surrounded by three bidentate BH_4-groups with AlH_2B planes perpendicular to the AlB_3 plane.

Decomposition of $Al(BH_4)_3$ starts at 150 °C and has a first order kinetics that is not affected by the presence of hydrogen.[14] Calculated heat of formation is estimated as –5.5 kJ/mol H_2 with the zero-point energy correction.[13]

Scandium borohydride Sc(BH₄)₃. Surprisingly little is known about scandium borohydride $Sc(BH_4)_3$. Solvates $Sc(BH_4)_3 \cdot 2THF$ and $Sc(BH_4)_3 \cdot DME$ are known but these complexes can not be desolvated. Ball-milling of $ScCl_3$ and $LiBH_4$ yields an amorphous product with ν(B–H) vibration in the range 2200–2500 cm⁻¹ in the Raman spectrum.[15] The decomposition of this product starts above 150 °C and has a maximum at ~260 °C.[15]

Titanium borohydride Ti(BH₄)₃ was prepared by the reaction of $LiBH_4$ with $TiCl_4$[39] or $TiCl_3$[40] (Ti fluoride salts do not react) and isolated by low temperature vacuum sublimation. $Ti(BH_4)_3$ is a white volatile solid. Electron diffraction in the gas phase showed a monomer molecule with tridentate BH_4-groups. Based on its physical properties, the bonding in titanium borohydride crystals should be similar to that in molecular crystals of $Al(BH_4)_3$. $Ti(BH_4)_3$ is thermally unstable and decomposes to TiB_2, H_2, and B_2H_6 at 20 °C.[16]

Manganese borohydride Mn(BH₄)₂ was isolated only as a solvate with ethers or amines. Attempts to desolvate $Mn(BH_4)_2 \cdot nL$ resulted in its decomposition with the ligand's destruction.[41]

Zirconium borohydride Zr(BH₄)₄ is conveniently prepared by mechanochemical synthesis using $NaZrF_5$ and $ZrCl_4$ in combination with $Al(BH_4)_3$ and alkali metal borohydrides.[39] $Zr(BH_4)_4$ decomposition produces a solid with the composition $ZrB_{2.76–3.74}$.[17] The only crystalline phase in this product is ZrB_2, therefore the rest is probably amorphous boron. The difference in the B:Zr ratio in starting material and products points to the possible evolution of diborane during pyrolysis.

Thermodynamic Properties of Metal Borohydrides

The heat of dehydrogenation (or reverse reaction of hydrogenation) is a very important parameter of hydrogen storage materials. It is desirable that this value is about 40 kJ/mol H_2 to provide a reasonable part of lower heating value (LHV), and a reasonable equilibrium hydrogen pressure at 80–120 °C. Despite the long history of metal borohydrides, only a few data on their thermodynamic properties has been published in the open literature.[8] Direct calorimetric measurements of very reactive and volatile compounds are very challenging. Therefore, calculation of thermodynamic characteristics of metal borohydrides using density functional theory (DFT) became a common practice. These calculations have a good correlation with experimental data only if the crystal structure of compounds is known (including coordinates of hydrogen atoms). It should be noted that standard enthalpy of formation (reverse of reaction 14) and enthalpy of dehydrogenation (ΔH_{des}) may not have the same absolute value because dehydrogenation of $M(BH_4)_n$ may occur with the formation of the corresponding metal hydride or/and boride (compare Eqs. 7, 12 and 14). Known data on enthalpies of decomposition of $M(BH_4)_n$ are given in Table 1. It was proposed that there is a linear relationship between heat of formation of $M(BH_4)_n$ and electronegativity of the metal.[15] There is also an almost linear correlation between desorption temperature and estimated ΔH_{des}.[15]

$$M(BH_4)_n \longrightarrow M + nB + 2n\,H_2 \quad (14)$$

A very promising concept of destabilization of metal borohydrides using the formation of metal borides was suggested by Vajo et al.[5] The concept is based on the use of stable borides (MgB_2,[5] AlB_2[6]), possibly in combination with lithium alloys (Li_7Sn_2, $Li_{0.3}Mg_{0.7}$)[4,42] to effectively decrease ΔH_{des} (Eqs. 15–17). Formation of borides instead at elemental boron decreases reaction enthalpies by 10–25 kJ/mol H_2, which in turn

For questions, product data, or new product suggestions, please contact the Materials Science team at matsci@sial.com.

Order: 1.800.325.3010 Technical Service: 1.800.231.8327

ALDRICH®

is related to the decrease of the decomposition temperature by 150–250 °C (Table 1). To further lower the decomposition temperature, it was proposed to use substitution of Li^+ for cations such as Mg^{2+}.[43] This idea worked well for $LiNH_2$, which has the structure similar to $Mg(NH_2)_2$,[44] but in the case where crystal structures are different, it may not work.

$$2\ LiBH_4 + MgH_2 \longrightarrow 2\ LiH + MgB_2 + 4\ H_2 \qquad (15)$$

$$2\ LiBH_4 + Al \longrightarrow 2\ LiH + AlB_2 + 3\ H_2 \qquad (16)$$

$$7\ LiBH_4 + 1.75\ Mg_2Sn + 0.25\ Sn \longrightarrow 2\ Li_7Sn_2 + 3.5\ MgB_2 + 14\ H_2 \quad (17)$$
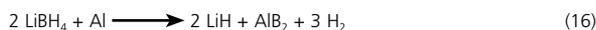
Metal Borohydrides as Hydrogen Storage Materials

The following major challenges in the chemistry of $M(BH_4)_n$ must be solved before their commercial use as hydrogen storage materials: high temperature of dehydrogenation, lack of reversibility of the dehydrogenation reaction, slow kinetics of dehydrogenation and hydrogenation, evolution of diborane during dehydrogenation, and, finally, high cost of borohydrides. Taking into account these considerations and hydrogen content, the most promising materials for hydrogen storage are borohydrides of lithium, magnesium, and calcium and their compositions. At first sight, $Ca(BH_4)_2$ has low gravimetric hydrogen storage capacity, but its volumetric capacity is higher than that of $LiBH_4$ and comparable with $Mg(BH_4)_2$ (Table 1).

It was found that mixing $LiBH_4$ with silica powder (3:1) substantially decreased its decomposition temperature.[25] In this case hydrogen release starts at 200 °C and occurs in two steps with a maximum at 320 °C (broad desorption peak) and 453 °C (sharp peak). The mechanism of such catalytic action is presently unclear. As mentioned above, destabilization of $M(BH_4)_n$ due to boride formation substantially decreases decomposition position temperature. However, the observed temperature decrease is noticeably lower than that predicted by thermodynamics (Table 1). Probably, the kinetics of metal boride formation is slow and dehydrogenation occurs by parallel pathways with formation of both metal boride and elemental boron.

Borohydride formation by reaction of hydrogen with boron and hydrides of Li, Na, Mg, and Ba at 600–700 °C was described in patent literature.[21] Reaction with LiH requires 150 bar H_2 while in the case of MgH_2 a much higher pressure (800 bar) is needed. The use of MgB_2 (instead of B) with LiH decreases the hydrogenation pressure and temperature to 100 bar and 300 °C, respectively.[5] Hydrogenation of the mixtures of MgB_2 with hydrides of sodium and calcium allowed synthesis of $NaBH_4$ and $Ca(BH_4)_2$ at 200 bar and 300 °C.[4] Reaction time is rather long (24 h) even at 350 bar and 400 °C.

It should be noted that effective catalysts of dehydrogenation/ hydrogenation of metal borohydrides, like titanium catalysts for $NaAlH_4$,[1] have not been found yet (except silica for $LiBH_4$).[25] Further efforts to make the decomposition of $Mg(BH_4)_2$ reversible as well as improving the reaction kinetics of Li and Ca borohydrides should concentrate on the development of catalysts for these reactions.

References:

(1) Bogdanovič, B.; Schwickardi, M. *J. Alloys Compounds* **1997**, *253/254*, 1. (2) Konovalov, S. K.; Bulychev, B. M. *Inorg. Chem.* **1995**, *34*, 172. (3) Stasinevich, D. S.; Egorenko, G. A. *Zh. Neorg. Khim.* **1968**, *13*, 654. (4) Barkhordarian, G.; Klassen, T.; Dornheima, M.; Bormann, R. *J. Alloys Compounds* **2007**, *in press*. (5) Vajo, J. J.; Skeith, S. L.; Mertens, F. *J. Phys. Chem. B* **2005**, *109*, 3719. (6) Cho, Y. W.; Shim, J.-H.; Lee, B.-J. *Calphad* **2006**, *30*, 65. (7) Czujko, T.; Varin, R. A.; Wronski, Z.; Zaranski, Z.; Durejko, T. *J. Alloys Compounds* **2007**, *427*, 291. (8) Sarner, S. F. *Propellant Chemistry*; 1st ed.; Reinhold Publishing: NY, 1966. (9) Kuznetsov, V. A.; Dymova, T. N. *Russ. Chem. Bull.* **1971**, *20*, 204. (10) Konoplev, V. N., Sizareva, A.S. *Koord. Khim.* **1992**, *18*, 508. (11) Miwa, K.; Aoki, M.; Noritake, T.; Ohba, N.; Nakamori, Y.; Towata, S.-i.; Zuttel, A.; Orimo, S.-i. *Phys. Rev. B* **2006**, *74*, 155122. (12) Jeon, E.; Cho, Y. *J. Alloys Compounds* **2006**, *422*, 273. (13) Miwa, K. *J. Alloys Compounds* **2007**, *in press*. (14) Brokaw, R. S.; Pease, R. N. *J. Am. Chem. Soc.* **1952**, *74*, 1590. (15) Nakamori, Y.; Miwa, K.; Ninomiya, A.; Li, H.; Ohba, N.; Towata, S.-i.; Zuttel, A.; Orimo, S.-i. *Phys. Rev. B* **2006**, *74*, 045126. (16) Volkov, V. V.; Myakishev, K. G. *Izv. Sibirskogo Otd. Akad. Nauk SSSR, Ser. Khim. Nauk* **1977**, 77. (17) Andrievskii, R. A.; Kravchenko, S. E.; Shilkin, S. P. *Inorganic Materials (Translation of Neorganicheskie Materialy)* **1995**, *31*, 965. (18) Schlesinger, H. I.; and Brown, H.C. *J. Am. Chem. Soc.* **1940**, *62*, 3429. (19) Schlesinger, H. I. et al. *J. Am. Chem. Soc.* **1953**, *75*, 186. (20) Buchner, W.; Niederprum, H. *Pure & Appl. Chem.* **1977**, *49*, 733. (21) Goerrig, D.: DE1077644, 1957. (22) Koster, R.; (Studiengesellschaft Kohle m. b. H.). DE1080983, 1960. (23) Volkov, V. V.; Myakishev, K. G. *Inorganica Chimica Acta* **1999**, *289*, 51. (24) Fedneva, E. M.; Alpatova, V. I. *Zh. Neorg. Khim.* **1964**, *9*, 1519. (25) Zuttel, A.; Rentsch, S.; Fischer, P.; Wenger, P.; Sudan, P.; Mauron, P.; Emmenegger, C. *J. Alloys Compounds* **2003**, *356–357*, 515. (26) Stasinevich, D. S.; Zhigach, A. F.; Antonov, I. S.; Ul'yanova, N. S. *Zh. Fiz. Khim.* **1976**, *50*, 3109. (27) Burg, A. B.; Schlesinger, H. I. *J. Am. Chem. Soc.* **1940**, *62*, 3425. (28) Schlesinger, H. I.; Brown, H. C.; Hyde, E. K. *J. Am. Chem. Soc.* **1953**, *75*, 209. (29) Lipscomb, W. N.; Marynick, D. *J. Am. Chem. Soc.* **1971**, *93*, 2322. (30) Wiberg, E.; Bauer, R. *Z. Naturforsch.* **1950**, *5b*, 397. (31) Plešek, J.; Heřmánek, S. *Coll. Czech. Chem. Comm.* **1966**, *31*, 3845. (32) Konoplev, V. N.; Bakulina, V. M. *Izv. Akad. Nauk SSSR, Ser. Khim.* **1971**, 159. (33) Rijssenbeek, J., Gao, Y., Soloveichik, G. Hanson, J. C. In *2006 MRS Fall Meeting. Symposium Z: Hydrogen Storage Technologies*: Boston, MA, 2006, p Z2.4. (34) Wiberg, E.; Hartwimmer, R. *Z. Naturforsch.* **1955**, *10b*, 295. (35) Wiberg, E.; Noth, H.; Hartwimmer, R. *Z. Naturforsch.* **1955**, *10b*, 292. (36) Mikheeva, V. I.; Titov, L. V. *Zh. Neorg. Khim.* **1964**, *9*, 789. (37) Hinkamp, J. B.; Hnizda, V. *Ind. Eng. Chem.* **1955**, *47*, 1560. (38) Semenenko, K. N.; Kravchenko, O. V.; Lobkovskii, E. B. *J. Struct. Chem.* **1972**, *13*, 508. (39) Hoekstra, H. R.; Katz, J. J. *J. Am. Chem. Soc.* **1949**, *71*, 2488. (40) Volkov, V. V.; Myakishev, K. G. *Izv. Akad. Nauk SSSR, Ser. Khim.* **1987**, 1429. (41) Makhaev, V. D.; Borisov, A. P.; Karpova, T. P.; Petrova, L. A. *Zh. Neorg. Khim.* **1995**, *40*, 1641. (42) Yu, X. B.; Grant, D. M. and Walker, G. S. *Chem. Commun.* **2006**, 3906. (43) Miwa, K.; Ohba, N.; Towata, S.-i.; Nakamori, Y.; Orimo, S.-i. *Phys. Rev. B* **2004**, *69*, 245120. (44) Orimo, S.; Nakamori, Y.; Kitahara, G.; Miwa, K.; Ohba, N.; Noritake, T.; Towata, S. *Applied Physics A: Materials Science & Processing* **2004**, *79*, 1765.

Metal Borohydrides for H_2 Storage

Boron-Based Materials for Hydrogen Storage Applications

Name	Mol. Formula	Hydrogen cont. wt.%	Properties	Purity (%)	Prod. No.
Lithium borohydride	$LiBH_4$	13.9	Decomposition temp. 470 °C moisture sensitive, toxic	>90	**222356-1G** **222356-10G** **222356-50G**
				>95	**62460-5G-F** **62460-25G-F**
Potassium borohydride	KBH_4	7.4	Decomposition temp. 500 °C moisture sensitive, toxic	98	**P4129-100G**
				99.9	**438472-5G** **438472-25G**
				≥98	**455571-5G** **455571-100G** **455571-500G**
				≥97.0	**60080-25G** **60080-100G**
Sodium borohydride	$NaBH_4$	10.6	Decomposition temp. 595 °C reacts with water stable in basic aqueous solutions	>98	**452165-100G** **452165-500G**
					452173-100G **452173-500G**
				98	**452874-25G** **452874-100G** **452874-500G**
				≥98.5	**452882-25G** **452882-100G** **452882-500G** **452882-2KG**
				99.99	**480886-25G** **480886-100G**
Calcium borohydride bis(tetrahydrofuran) complex	$Ca(BH_4)_2 \cdot 2C_4H_8O$	11.5 (unsolvated)	Decomposition temp. 360 °C (after desolvatation at 190 °C in vacuum) soluble in water without decomposition	>96	**389986-1G** **389986-5G**
				>98	**21057-1G** **21057-5G**
Magnesium boride	MgB_2		Stable Used as catalyst/additive	97	**553913-5G** **553913-25G**

For details, visit **sigma-aldrich.com/hydrogen**.

Metal Borohydrides for H2 Storage

Order: 1.800.325.3010 Technical Service: 1.800.231.8327

For questions, product data, or new product suggestions, please contact the Materials Science team at matsci@sial.com.

ALDRICH

Mechanical Processing in Hydrogen Storage Research and Development

Dr. Viktor P. Balema
Sigma-Aldrich Materials Science

Introduction

Storing hydrogen in solids—hydrides, composite materials or metal-organic frameworks—offers a unique opportunity for its convenient and safe use in automotive, portable and other applications. Unfortunately, none of the materials currently on the market satisfy the needs of end users, which explains the growing interest and investments into hydrogen storage related research and development.[1,2]

Throughout this issue, leading experts in the field discuss recent experimental results and ideas associated with hydrogen storage applications. Complementing these reports, the article below addresses an experimental approach, which proved to be indispensable in basic and applied hydrogen storage R&D[2]—the preparation and modification of hydrogen rich molecular and ionic materials using high-energy mechanical milling.

Mechanically Induced Conversion of Metal Hydrides

Although mechanical milling has been routinely used in processing of solids for hundreds of years, systematic studies into its chemical effects began relatively recently.[3] By the end of 20th century, mechanical processing by milling, also known as mechanical alloying or mechanochemistry, matured into an experimental technique routinely used in the preparation of metal alloys, ceramics and composites.[4] It has also become indispensable for the preparation and processing of hydrogen-rich solids, including metal hydrides.[2,4]

Usually, mechanochemical experiments are carried out in a planetary or vibro-mill in a tightly sealed container (**Figure 1**) that can be loaded and unloaded under inert gas in a glove box.

In a typical procedure, pure solids or mixtures are charged into a milling vial and ball-milled for a defined period of time. The material is then recovered from the vial and investigated using an appropriate solid-state analytical technique such as x-ray or neutron diffraction, magic angle spinning solid-state nuclear magnetic resonance (MAS NMR), IR- or UV-spectroscopy, thermal analysis, and others. It is worth noting that MAS NMR has recently proven to be particularly efficient in monitoring chemical processes in metal hydrides[5,6] and other solids.[7]

Metal Hydrides

Use of the mechanochemical technique enabled the discovery of chemical processes that can take place in metal hydrides in the solid state. It turns out that solid-state chemistry of aluminum- and boron-based hydrides is quite as rich as their chemistry in solution. For example, ball milling of alkali metal aluminohydrides with binary alkali metal hydrides allows for a convenient preparation of hexahydroaluminates, which are hardly accessible through the wet-chemistry synthetic routes.
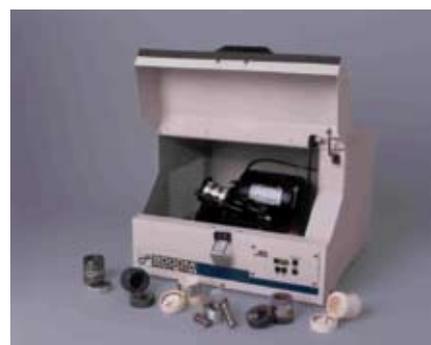
Figure 1. A planetary mill Pulverisette 5 / 4, Fritsch (top) and a shaker mill Spex 8000M (bottom). Images provided by manufacturers.

Moreover, it became evident that numerous chemical reactions in metal—aluminum or boron—hydrogen systems do not, in fact, require a liquid phase and can be successfully run under solvent-free conditions (Eqs. 1–6).

$$MH + AlH_3 \longrightarrow MAlH_4 \tag{1}[8,9]$$

$$2MH + 2Al + 3 H_2 \longrightarrow 2MAlH_4 \tag{2}[10,11]$$

$$MAlH_4 + 2MH \longrightarrow M_3AlH_6 \tag{3}[12,13]$$

$$M_3AlH_6 + 2AlH_3 \longrightarrow 3MAlH_4 \tag{4}[8,9]$$

$$M = Li,\ Na$$

$$TiCl_3 + 3LiBH_4 \longrightarrow Ti(BH_4)_3 + 3LiCl \tag{5}[14]$$

$$UCl_4 + 4LiBH_4 \longrightarrow U(BH_4)_4 + 4LiCl \tag{6}[14]$$
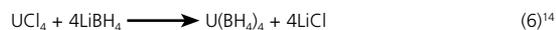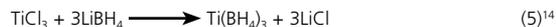
The mechanochemical technique has also helped to identify some of the titanium-species that form during doping of alkali metal aluminohydrides or magnesium hydride with Ti-salts (Eqs. 7,8).[15–17] Another result of mechanochemical studies is the discovery of Ti-catalyzed decompositions of $LiAlH_4$ at room temperature upon mechanical milling.[18]

$$nMAlH_4 + TiCl_n \longrightarrow nMCl + Al + TiAl_3 + [TiH]_x(traces) + H_2 \tag{7}[15,16]$$

$$M = Li,\ Na;\ n = 3,4$$

$$MgH_2 + TiCl_3 \longrightarrow MgCl_2 + TiH_2 \tag{8}[17]$$

Along with fundamental studies into the solid-state reactivity of metal and boron hydrides, solvent-free mechanochemistry has been successfully used in the preparation of binary and complex metal hydrides (Eqs. 9–12) as well as low molecular weight gases such as the extremely toxic diborane (Eq. 13). The latter can also form as a by-product in other mechanically induced processes involving alkali metal borohydrides and transition metal salts[14] (for more examples see the article by G. Soloveichik on page 11).

Mechanical Processing in H₂ Storage

$$M + H_2 \longrightarrow MH_x \qquad\qquad (9)^{19}$$

M = Mg, Ti, Zr, Nb   x=1–2

$$MgCl_2 + 3LiAlH_4 \longrightarrow LiMg(AlH_4)_3 + 2LiCl \qquad (10)^{20}$$

$$3LiAlD_4 + AlCl_3 \longrightarrow 4AlD_3 + 3LiCl \qquad\qquad (11)^{21}$$

$$MgH_2 + Co \longrightarrow MgCoH_5 \qquad\qquad (12)^{22}$$

$$2NaBH_4 + SnCl_2 \longrightarrow 2NaCl + Sn + 2H_2 + B_2H_4 \qquad (13)^{14}$$
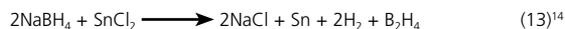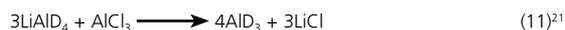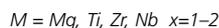
A number of other mechanically induced transformations involving metal alloys, amides, nitrides, and nano-materials has been published during the last decade. Due to the limited size of this publication, they will be discussed in the future.

Mechanism of Mechanochemical Reactions

Even a brief glimpse at the previous paragraphs is sufficient to realize the extreme diversity and complexity of solid-state processes that can occur in a crystalline solid trapped between steel or ceramic balls, colliding in a tightly-closed vial. Indeed, high-energy ball-milling brings about a broad variety of defects including cracks, pores, dislocations, vacancies, new surfaces, grain, twin boundaries, and others. Prolonged milling can also destroy crystallinity of the material leading to its complete or partial amorphization.[23] Changes in a solid crystalline material under mechanical stress start with its elastic deformation, which disappears once the load is lifted. If, however, the load increases, the elastic deformation transforms into an irreversible plastic deformation, which is followed by the fracture and/or amorphization of the material. Plastic deformations normally occur under shear stress, parallel to the face of the material, as opposed to brittle fractures that take place under normal stress perpendicular to the face (**Figure 2**).
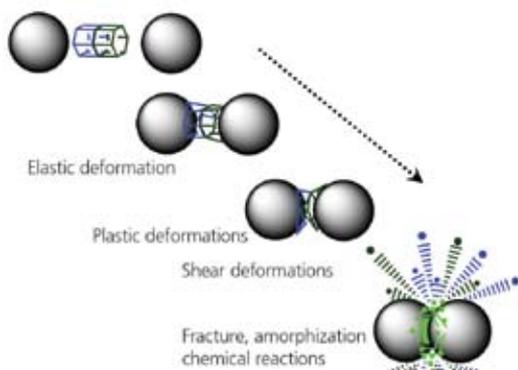
Figure 2. Changes in the material trapped between colliding balls in a ball mill.

Thus, physicochemical effects of mechanical milling include breaking crystallinity, creating new surfaces, and mass transfer (mixing).

The constant formation of a new surface and mass transfer are major factors responsible for the enhanced reactivity of metals toward hydrogen under ball-milling (Eq. 9). At the same time, these effects cannot be solely responsible for solid-to-solid reactions discussed previously as well as for the transformations in other molecular and ionic solids shown in **Figure 3**.[24–26]
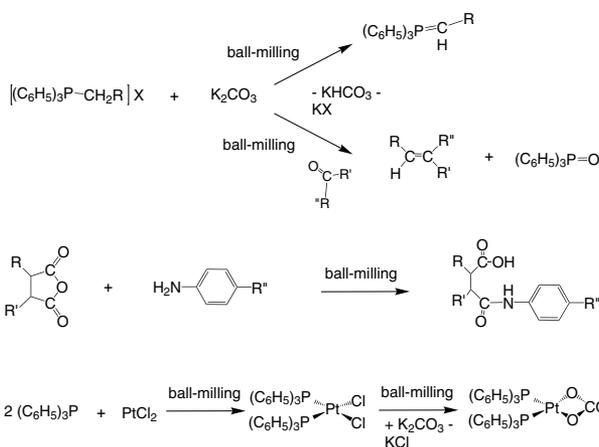
Figure 3. Mechanically induced reactions of organic and metal-organic solids.

These studies revealed that mechanochemical reactions in molecular and ionic solids are not temperature-driven processes. In a number of cases, the temperature increase in the material during milling is well below their melting or decomposition points.[24–26] In addition, the theoretical analysis of a ball-milling process in a commercial Spex-type shaker mill revealed a moderate temperature effect (~60 °C). According to the same study, the pressure generated in the solid, trapped between two colliding balls, can rise as high as several GPa,[27,28] thus facilitating genuine ultra-high pressure activated processes.[29]

Some additional insight into the nature of mechanically induced chemical reactions is provided by the photochemical dimerization of anthracene (**Figure 4**). It occurs readily in solution but does not take place in the solid state because of the unfavorable orientation of anthracene molecules in the crystal. No photochemical reaction is observed when crystalline anthracene is subjected to high hydrostatic pressure up to 10 GPa. However, once external pressure is combined with a shear stress, the photochemical reaction becomes possible. Apparently, the high pressure combined with the shear stress not only reduces the distance between molecules but also changes their orientation in the solid, thus making the reaction possible.[30,31]
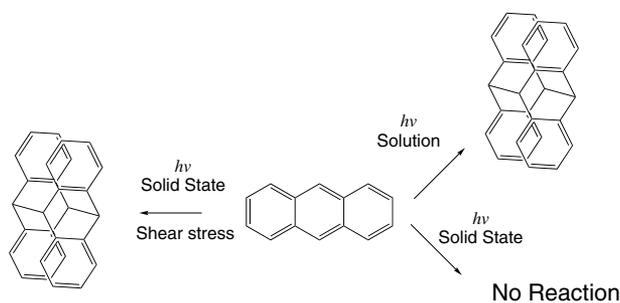
Figure 4. Photochemical dimerization of anthracene.

In conclusion, mechanochemistry has proven to be an extremely useful tool for the preparation of novel materials as well as for the investigation of chemical transformations that can take place in solids under solvent-free conditions. Although the exact mechanism of mechanochemical phenomena should be determined on a case-by-case basis, it appears that mechanochemical processes in solids are primarily driven by structural changes and high pressure, generated in the material during milling. The crystal structure, lattice energy, and chemical reactivity of the material govern the magnitude of the energy input required for such processes to occur.

References:

(1) Hydrogen Posture Plan, the U.S. Department of Energy, 2006. (2) http://www.hydrogen.energy.gov/annual_progress06.html (3) Heinicke, G., *Tribochemistry*; Academie Verlag: Berlin, 1984. (4) Suryanarayana, C. *Progr. Materials Sci.* **2001**, *46*, 1. (5) Bowman, R. C.; Hwang, S.-J. *Material Matters* **2007**, *Vol 2 No 2*, 29. (6) Balema, V. P.; Balema, L. *Phys. Chem. Chem. Phys.* **2005**, *7*, 1310. (7) Minkel, J. R. *New Scientist* **2002**, *174*, 18. (8) Dymova, T. N.; Aleksandrov, D. P.; Konoplev, V. N.; Silina T.; Kuznetsov, N. T. *Russian J. Coord. Chem.* **1993**, *19*, 491. (9) Chaudhuri, S.; Graetz, J.; Ignatov, A.; Reilly, J. J.; Muckerman, J. T. *J. Am. Chem. Soc.* **2006**, *128*, 11404. (10) Bellosta von Colbe, J. M.; Felderhoff, M.; Bogdanović, B.; Schüth, F.; Weidenthaler, C. *Chem. Commun.*, **2005**, 4732. (11) Kojima, Y.; Kawai, T.; Haga, T.; Matsumoto, M.; Koiwai, A. *J. Alloys Compds.* **2007**, On the web 7 February 2007 (12) Hout, J.; Boily, S.; Gunther, V.; Schulz, R. *J. Alloys Compds.* **1999**, *283*, 304. (13) Balema, V. P.; Pecharsk, V. K.; Dennis, K. W. *J. Alloys Compds.* **2000**, *313*, 69. (14) Volkov, V. V.; Myakishev, K. G. *Inorg. Chim. Acta* **1999**, *289*, 51. (15) Balema, V. P.; Wiench, J. W.; Dennis, K. W.; Pruski, M.; Pecharsky, V. K. *J. Alloys Compds.* **2001**, *329*, 108. (16) Herberg, J. L.; Maxwell, R. S.; Majzoub, E. H. *J. Alloys Compds.* **2005**, *417*, 39. (17) Charbonnier, J.; de Rango, P.; Fruchart, D.; Miraglia, S.; Pontonnier, L.; Rivoirard, S.; Skryabina, N.; Vulliet, P. *J. Alloys Compds.* **2004**, *383*, 205. (18) Balema, V. P.; Dennis, K. W. ; Pecharsky, V. K. *Chem. Commun.* **2000**, 1665. (19) Chen, S.; Williams, *J. Materials Science Forum 225/227*; TransTech Publications Inc.: Stafa-Zurich, 1996; p 881. (20) Mamathab, M.; Bogdanović, B.; Felderhoff, M.; Pommerin, A.; Schmidt, W.; Schüth, F.; Weidenthaler, F. *J. Alloys Compds.*, **2006**, *407*, 78. (21) Brinks, H. W., et al. *J. Phys. Chem.* **2006**, *110*, 25833. (22) Chen J., *J. Mater. Sci.* **2001**, *36*, 5829. (23) Balema, V. P.; Wiench, J. W.; Dennis K. W.; Pruski M.; Pecharsky V. K. *J. Am. Chem. Soc.* **2002**, *124*, 6244. (24) Balema, V. P.; Wiench, J. W.; Dennis, K. W.; Pruski, M.; Pecharsky, V. K. *Chem. Commun* **2002**,1606. (25) Boldyrev, V. V. *Reactivity of Solids: Past Present and Future*; IUPAC and Blackwell Science Ltd.: Oxford, 1996. (26) Takacs, L. *Progr. Materials Sci.* **2002**, *47*, 355. (27) Maurice, D. R.; Courtney T. H., *Metall. Trans. A*, **1990**, *21*, 286. (28) Koch, C. C., *Int. J. Mechanochem. Mech. Alloying*, **1994**, *1*, 56. (29) *High Pressure Molecular Science, NATO Science Series, E358*; Ed. Winter R.; Jonas J.; Kluwer Academic Publishers: Dordrecht, Boston, London, 1999. (30) Oehzelt, M.; Resel R. *Phys. Rev. B.* **2002**, *66*, 174104. (31) Politov, A. A.; Fursenko, B. A.; Boldyrev, V. V. *Doklady Phys. Chem.* **2000**, *371*, 28.

Research Kits for Hydrogen Storage Applications

Sigma-Aldrich has assembled groupings of products for hydrogen storage applications to assist you in designing research-scale experiments. These "virtual kits" are offered at a special group price. For ease of ordering, simply request these product groupings by the designated kit number. Please note that the components assigned to each of these "virtual kits" will be delivered as separate units.* They may also be ordered separately using the component Prod. No. as your needs require.

Hydrogen Storage Materials for Research—686093–1KT*

The materials for hydrogen storage research listed below are offered as 10 g units. Hydrogen content, XRD plots and metal purity data are available for all components.

Name	Mol. Formula	Hydrogen cont. (wt %)	Purity (%)	Prod. No.
Lithium amide	$LiNH_2$	8.7	>95	**686050-10G**
Sodium amide	$NaNH_2$	5.1	>95	**686042-10G**
Lithium nitride	Li_3N		>95	**399558-10G**
Lithium aluminum hydride	$LiAlH_4$	10.5	>97	**686034-10G**
Sodium aluminum hydride	$NaAlH_4$	7.4	>97	**685984-10G**
Lithium hydride	LiH	12.6	>95	**201049-10G**
Sodium hydride	NaH	4.1	>95	**223441-10G**
Calcium hydride	CaH_2	4.7	>95	**213322-10G**
Lithium borohydride	$LiBH_4$	13.9	>95	**686026-10G**
Sodium borohydride	$NaBH_4$	10.6	>95	**686018-10G**
Borane-ammonia complex	$H_3N–BH_3$	19.5	>95	**287717-10G**
Magnesium hydride	MgH_2	7.6	98	**683043-10G**

Catalysts for Hydrogen Storage Research—686107–1KT*

The catalysts for hydrogen storage research listed below are offered as 1 g units. XRD and metal purity data are available for all components.

Name	Mol. Formula	Hydrogen cont. (wt %)	Purity (%)	Prod. No.
Niobium(V) oxide	Nb_2O_5		99	**208515-1G**
Titanium(III) chloride	$TiCl_3$		99	**686085-1G**
Titanium(II) hydride	TiH_2	4.0	98	**686069-1G**
Zirconium(II) hydride	ZrH_2	2.1	99	**208558-1G**
Vanadium(III) chloride	VCl_3		97	**208272-1G**
Scandium(III) chloride	$ScCl_3$		99	**686077-1G**

For more information about these and other related materials, please visit **sigma-aldrich.com/hydrogen**.

*Products do not ship in a single package.

Mechanical Processing in H₂ Storage

ALDRICH®

sigma-aldrich.com

Nanoarchitecture of Protective Coatings for Air Sensitive Metal Hydrides
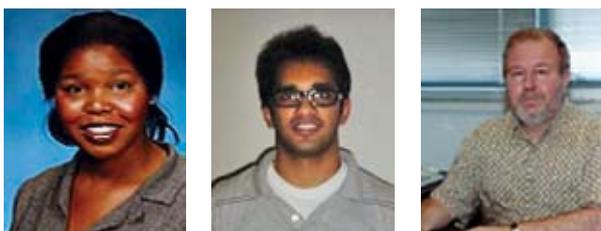
Dr. Tabbetha Dobbins, Vimal Kamineni, and Dr. Yuri Lvov
Institute for Micromanufacturing, Louisiana Tech University

Introduction

Hydrogen storage materials are being considered for safe on-board vehicle storage of H_2 gas used to power proton exchange membrane fuel cells. There are various methods for storing hydrogen,[1] which include high pressure storage in aluminum containers,[2] chemisorbed onto metal hydrides[3] and physisorbed onto carbon-based materials.[4] Metal hydrides are viewed as one of the most feasible storage method because they are low volume containment vehicles for H_2 gas, and they show promise for H_2 desorption under mild conditions.

Metal hydrides are compounds comprised of one or more metals that contain anionic hydrogen (H^-) in their lattice. There are a vast number of metal hydrides that can be synthesized, but the prevalent scope of interest is in the lighter metal hydrides (the weight % of hydrogen increases as the molecular weight of the metal hydride decreases). Of these light metal hydrides, sodium aluminum hydride ($NaAlH_4$, Aldrich Prod. No. **357472**), lithium aluminum hydride ($LiAlH_4$, Aldrich Prod. No. **199877**), lithium hydride (LiH, Aldrich Prod. No. **201049**), and sodium hydride (NaH Aldrich Prod. No. **223441**) have high gravimetric storage capacity for hydrogen, but are also reactive in air and moisture-rich environments.[5]

Our research impacts on the hydrogen energy economy through the development of "smart" nanofilms for the protection of metal hydrides against air and moisture, while permitting release of hydrogen gas through these semi permeable nanofilms. Future generations of these films may have catalytic metals—known to enhance the dehydrogenation reaction[6]—embedded within for the purpose of controlled release of catalyst to the hydride particle surface. Our nanofilms for encapsulating metal hydrides are layer-by-layer electrostatic self-assembled films.

Layer-by-layer thin films are comprised of polyelectrolyte layers each on the order of 2 nm thickness.[7,8] The layer-by-layer self-assembly technique can be used to deposit conformal, multilayer nanofilms onto planar surfaces and colloidal particles. Film growth is made possible by coulumbic attraction between the polycation and the polyanion at the surface to be coated. The working medium for self-assembly is typically water or acetone-water mixtures.[9] However, water as a solvent cannot be used to coat the water-sensitive metal hydrides. For metal hydrides, pure formamide was used as a solvent for the self-assembly of films.[10]

Layer-by-Layer Self-Assembly

Layer-by-layer electrostatic self-assembly coating of nanofilms was performed onto sodium aluminum hydride powders using formamide as the working medium. The polyanions are polystyrene sulfonate [(PSS) (MW 70,000) (Aldrich Prod. No. **243051**)] and the polycations are polyallylamine hydrochloride [(PAH) (MW 15000) (Aldrich Prod. No. **283223**)]. **Figure 1** shows schematically the layer-by-layer self-assembly of PSS and PAH films over sodium aluminum hydride. For deposition onto colloidal sodium aluminum hydride, the powders were suspended in formamide using concentrations of 20 mg/mL. For self-assembly, PSS and PAH in concentrations of 2 mg/mL were added to the colloidal suspension in the following manner. The surface charge on bare sodium aluminum hydride in formamide is positive. Thus, sodium aluminum hydride particles contained in formamide suspension were first exposed to the polyanion (PSS) for a period of fifteen minutes and subsequently to the polycations (PAH) for a period of fifteen minutes.
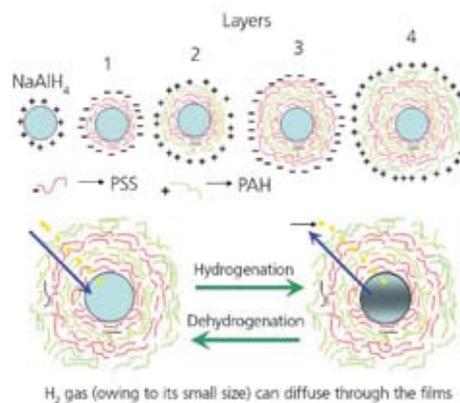
Figure 1. The growth of polymer films on sodium aluminum hydride.

After each exposure (and deposition of each film layer), the particles were removed from suspension by centrifugation and rinsed in formamide for a period of fifteen minutes. Zeta potential (Zetaplus, BIC) measurements were taken to observe the alternation in the surface charge after each polyelectrolyte exposure and formamide rinse. **Figure 2** shows schematically the process steps in the layer-by-layer self-assembly approach used. The processing steps were repeated until two bilayers of PSS and PAH (4 layers in total) overlaid the sodium aluminum hydride particle surface.

Follow the cycle for the next bilayers

→Pipette Supernatant

NaAlH$_4$ Particles

Formamide + PSS
(15 mins LbL Assembly)

Centrifuge
15 mins

After supernatant is removed, NaAlH$_4$ encapsulated by PSS monolayer resulting in (NaAlH$_4$)$_{PSS}$

Formamide + PAH
(15 mins LbL Assembly)

Centrifuge
15 mins

After supernatant is removed, (NaAlH$_4$)$_{PSS}$ is encapsulated by PAH monolayer resulting in one bilayer to yield (NaAlH$_4$)$_{PSS/PAH}$

Figure 2. The process of coating "smart" nanofilms onto sodium aluminum hydride.

One key indicator of the successful layering of alternately charged polyelectrolytes over colloidal particle surfaces during layer-by-layer self-assembly is the measured alternation in surface charge gained using zeta potential measurement (Zetaplus, BIC). **Figure 3** shows this surface charge reversal after each polyelectrolyte layer was deposited over sodium aluminum hydride. The surface charge measurements were taken after the formamide rinse step of our process. PSS is the polyanion and results in a zeta potential reading of a –60 mV after its first layering. PAH is the polycation resulting in a zeta potential reading of +16 mV after its first layering. The second bilayer comprised of PSS followed by PAH read surface charges of –75 mV and +16 mV, respectively.

An additional feature of the layer-by-layer self-assembly technique is its versatility in controlling total thickness of polyelectrolyte layers for the variety of polyelectrolytes that may be deposited over planar and colloidal particle surfaces. Inorganic clay flakes and nanoparticles of silica and titania may also be deposited over colloidal particles using layer-by-layer self-assembly. Our own work explores the versatility of the layer-by-layer technique in order to develop films of a protective nature and having the ability to prevent air and moisture from interacting with the reactive metal hydrides— thereby improving shelf life of these materials.
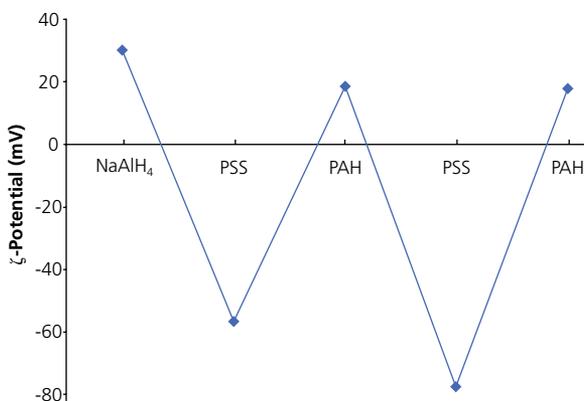
Figure 3. Zeta potential measurement from sodium aluminum hydride having PSS and PAH overlay films (two polymeric bilayers).

Protective Films Over Hydrides

The sodium aluminum hydride particles with two bilayers of PSS/PAH were carefully dried and imaged using an FESEM with energy dispersive spectroscopy (EDS) capabilities. The SEM image in **Figure 4** (left) shows a single sodium aluminum hydride particle having PSS/PAH overlay films. Energy dispersive x-ray mapping of carbon (Figure 4, right) reveals the conformal coverage of the polymeric films over the sodium aluminum hydride particle. In order to confirm that no reaction between the sodium aluminum hydride particles and the formamide working solvent had occurred, x-ray diffraction (XRD) of bare sodium aluminum hydride particles after a 24-hour soak in formamide was measured. **Figure 5** shows clearly that NaAlH$_4$ crystallographic peaks are consistent with the NaAlH$_4$ (indicated by red markers). Minor peaks occurring below 2θ=28° are from kapton tape used for protecting the sodium aluminum hydride during XRD measurement.
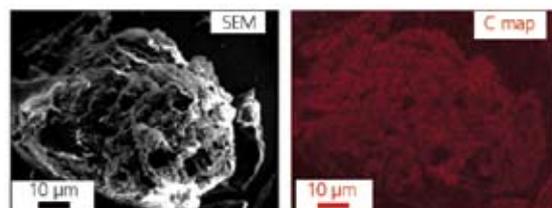
Figure 4. SEM and X-ray mapping of carbon (from nanofilms) on sodium aluminum hydride.
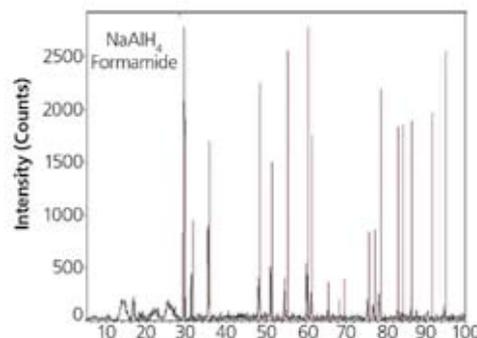
Figure 5. X-ray diffraction of NaAlH$_4$ after 24 hour soak in formamide— the working solvent.

Thus highly reactive and corrosive hydrides can be protected from air and moisture by encapsulating them within smart polyelectrolyte films. **Figure 6a** clearly shows complete and even coverage of PSS and PAH films (deposited onto planar surfaces from an aqueous working solvent). These films have surface defects due to inclusions of dust particles that may be removed from the solvents by submicron filtration. Studies to test the stability and permeability of PSS and PAH films to the gases H$_2$, O$_2$, and H$_2$O are underway and preliminary results are encouraging.
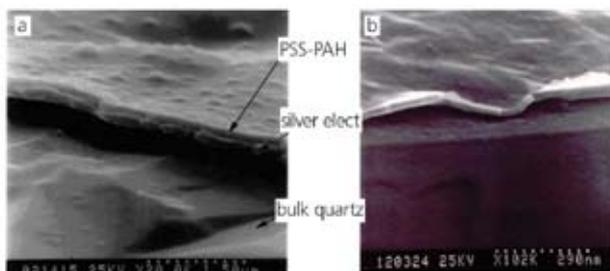
Figure 6. (a) (PSS/PAH)₆ multilayers on silver QCM. (b) Montmorillonite clay in alternation with PAH.

Future Outlook

Pure organic polymer films may not form very tight packing, so an alternative to forming air impermeable films is to introduce inorganic particles within the overlay films. Low permeability films over colloidal particles may be prepared from nanomaterials such as Montmorillonite clay flakes and inorganic TiO_2 and SiO_2 nanoparticles.

Clay Coating

Montmorillonite clay flakes of 1 nm thick and 500 nm cross-sections can be used to coat air and moisture sensitive metal hydrides. **Figure 6b** shows montmorillonite (negative surface charge) assembled through alternation with a polycation (PAH) providing a bilayer of 3.2 nm onto a Si substrate.[11,12] Using montmorillonite clay flakes, one can build a very tight organic-inorganic multilayer network. These clay/PAH films (Figure 6b) appear to be free of surface defects—compared with PSS/PAH films (Figure 6a). The internal structure of these multilayer films resembles paper mache—where gas diffusion may occur only by percolation through pores created by packing defects. Generally, such multilayers have a much lower permeability than organic films. The possibility for tunable permeability by controlling packing defects through varying self-assembly conditions is promising.

Nanoparticle Coating

Water-sensitive metal hydrides may also be coated with inorganic nanoparticles in alternation with organic polymer films. **Figure 7** demonstrates the coating of a 250 nm colloidal latex particle with 40 nm silica particles assembled in alternation with PSS/PAH.[13] The bare colloidal latex particle and the silica coated latex particle are shown in Figure 7. The protective nature of such films is demonstrated by the ability of a similarly architectured film to stabilize nifedipine from photoreaction.
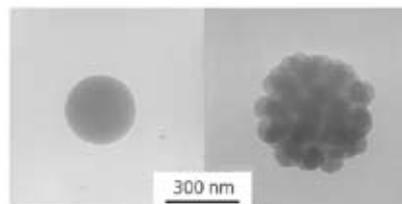
Figure 7. 250 nm diameter bare latex particle (left) and covered with 40-nm silica particle shell (PAH/PSS/PAH/silica) (right).

References:

(1) Zuttel, A. *Materials Today* **2003**, *6*, 24. (2) Fichtner, M. *Advanced Engineering Materials* **2005**, *7*, 443. (3) Sandrock, G. D.; Snape, E. *ACS Symposium Series* **1980**, 293. (4) Meregalli, V.; Parrinello, M. *Applied Physics A: Materials Science and Processing*, **2001**, *72*, 143. (5) Gross, K. *G-CEP Hydrogen Workshop*, April 14–15, **2003**. http://gcep.stanford.edu/events/workshops_hydrogen_04_03.html (accessed Feb. 23, 2007). (6) Bogdanovič, B.; Schwickardi, M. *Journal of Alloys and Compounds* **1997**, *253*, 1. (7) Lvov, Y.; Ariga, K.; Onda, M.; Ichinose, I.; Kunitake, T. *Colloids and Surfaces A: Physicochemical and Engineering Aspects* **1999**, *146*, 337. (8) Decher, G. *Science* **1997**, *227*, 1232. (9) Kuila, D.; Tien, M.; Lvov, Y.; McShane, M.; Aithal, R.; Singh, S.; Potluri, A.; Kaul, S.; Patel, D.; Krishna, G. *Proceedings of SPIE – The International Society for Optical Engineering* **2004**, *5593*, 267. (10) Kamineni, V.; Lvov, Y. M.; Dobbins, T. A. *Langmuir* Submitted. (11) Lvov, Y.; Ariga, K.; Ichinose, I.; Kunitake, T. *Langmuir* **1996**, *12*, 3038. (12) Tang, Z.; Kotov, N. A.; Magonov, S.; Ozturk, B. *Nature Materials* **2003**, *2*, 413. (13) Lu, Z.; Prouty, M. D.; Quo, Z.; Golub, V. O.; Kumar, C.S.S.R.; Lvov, Y. M. *Langmuir*, **2005**, *21*, 2042.

Acknowledgments

For questions, product data, or new product suggestions, please contact the Materials Science team at matsci@sial.com.

Metal Hydrides for Hydrogen Storage Applications

Name	Mol. Formula	Hydrogen cont. (wt %)	Properties	Purity (%)	Prod. No.
Calcium hydride	CaH_2	4.7	Decomposition temp. ~600 °C moisture sensitive	99.99	**497355-2G** **497355-10G**
				99.9	**558257-10G**
				95	**213322-100G** **213322-500G**
Lithium hydride	LiH	12.6	Decomposition temp. 720 °C moisture sensitive	95	**201049-5G** **201049-100G** **201049-500G**
Lithium aluminum hydride	$LiAlH_4$	10.5	Decomposition temp.: 150–175 °C (step 1) 180–224 °C (step 2) > 400 °C (step 3) extremely moisture sensitive	95	**199877-10G** **199877-25G** **199877-100G** **199877-1KG**
				>97	**62420-10G** **62420-50G** **62420-250G**
Sodium aluminum hydride	$NaAlH_4$	7.4	Decomposition temp.: 210–250 °C (step 1) 250–300 °C (step 2) > 400 °C (step 3) extremely moisture sensitive	97	**685984-10G**
				>90	**357472-25G**
Sodium hydride	NaH	4.1	Decomposition temp. 800 °C moisture sensitive	95	**223441-10G** **223441-50G** **223441-250G** **223441-1KG**
Titanium(II) hydride	TiH_2	4.0	Decomposition temp. 450–550 °C (step 1) 550–650 °C (step 2)	98	**209279-100G** **209279-500G**
Zirconium(II) hydride	ZrH_2	2.1	Decomposition temp. 600 °C	99	**208558-100G**

Nitrogen-Based Materials for Hydrogen Storage Applications

Name	Mol. Formula	Hydrogen cont. (wt %)	Properties	Purity (%)	Prod. No.
Ammonia	NH_3	17.6		99.99	**294993-170G**
Lithium amide	$LiNH_2$	8.7	Decomp. to Li_2NH >350 °C moisture sensitive	95	**213217-5G** **213217-100G** **213217-500G**
Sodium amide	$NaNH_2$	5.1	Decomp. 500 °C moisture sensitive	95	**71260-100G**
				95	**432504-25G** **432504-100G** **432504-500G**
				>90	**208329-50G** **208329-250G**
Aluminum nitride	AlN		Moisture sensitive	>98	**241903-50G** **241903-250G**
Calcium nitride	Ca_3N_2		Air/moisture sensitive	95	**415103-25G** **415103-100G**
Lithium nitride	Li_3N		Can be hydrogenated to Li_2NH and $LiNH_2$	95	**399558-5G** **399558-25G**
Magnesium nitride	Mg_3N_2		Air/moisture sensitive	>99.5	**415111-10G** **415111-50G**

For details visit **sigma-aldrich.com/hydrogen**.

Protective Nanocoatings for Metal Hydrides

Introducing HYDRNOL™: Organic Liquid Storage for Hydrogen

Dr. Esmaeel D. Naeemi, Dr. Dan Graham, and Barton F. Norton
Asemblon, Inc.

Introduction

There has been considerable discussion about the Hydrogen Economy and its promise of cars and trucks with clean burning internal combustion engines and highly-efficient fuel cells. California,[1–3] Iceland[4–6] and Norway[7–9] have all made commitments to Hydrogen Highways where hydrogen fueling stations will be available for the cars of tomorrow.

Unlike gasoline, hydrogen is abundant in the universe and can be generated from renewable sources of energy. However, hydrogen is the lightest element in the universe and has a low density, which makes it difficult to store and transport without bulky, heavy equipment. This is why the storage and transportation of hydrogen has been identified as the biggest challenge to establishing the Hydrogen Economy.

A number of key issues must be addressed to make this future a reality: sources of inexpensive hydrogen must be found, fuel cell technology must advance in capability and decrease in cost, and methods must be developed to efficiently store and transport hydrogen. Currently available methods for storing and delivering hydrogen fuel include compressed hydrogen, liquefied hydrogen, physical metal hydride storage, chemical hydride storage,[10–11] nanotube storage,[12–13] among others. Compressed and liquefied storage are primarily limited by costs. Methods needed to compress the hydrogen, as well as the large heavy tanks required to store the compressed/liquefied hydrogen add significantly to the cost. Additionally, these tanks pose a risk of explosion when positioned on-board of a moving vehicle. Hydride storage in metal hydrides is promising, but current methods are still expensive and heavy.[14]

Another alternative is to store hydrogen covalently in organic molecules. The advantage of storing hydrogen covalently as part of a molecule in comparison with physical trapping of hydrogen gas in a substrate is that the system does not require compression or cryogenic temperatures. An ideal solution would be the development of a liquid carrier. Such a liquid carrier for hydrogen would minimize the need for infrastructure changes, and eliminate the need for large, specialized storage containers. Furthermore, the world is accustomed to dealing with liquid fuel so adopting a new type of liquid fuel would be much easier than making major infrastructure and societal changes within the fuel industry.

*This paper addresses a new promising alternative for hydrogen storage and transportation: hydrogen stored covalently in an organic liquid carrier and released by interaction with a heated catalyst.

*Others have proposed using carbazoles[15] for hydrogen storage in organic molecules.

A Liquid Fuel for Hydrogen Storage

Asemblon, Inc. has developed a proprietary system for storing hydrogen. Asemblon's first United States patent will issue shortly. The Asemblon System consists of four components which are outlined in **Figure 1**:
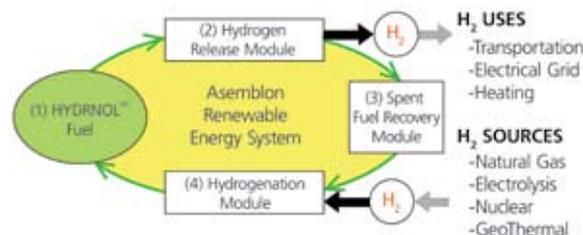
Figure 1. HYDRNOL™, along with the Hydrogen Release and Hydrogenation Modules, use patent-protected processes that are at the heart of the Asemblon System.

(1) Liquid Fuel HYDRNOL™

HYDRNOL™ is a hydrocarbon based organic molecule that is liquid at ambient temperature and atmospheric pressure. It can be distributed utilizing the established infrastructure of pipelines, barges, tankers and trucks. The molecule can be stored and pumped at traditional gasoline filling stations with minor modifications.

This fuel can be made from a variety of initial feed stocks including sweet and sour crude oil, and alcohols, including ethanol from biomass. Ethanol could be a primary source of this fuel with an estimated increase of only 10% to the cost of an ethanol production facility.

After releasing its hydrogen the spent fuel can be recycled by rehydrogenation back to the original molecule. During use, this fuel is kept in a dual-bladder gas tank either on-board of a vehicle or at a stationary site.

(2) Hydrogen Release Module

Inside the Hydrogen Release Module (HRM), the fuel comes in contact with a hot, high surface area catalyst and instantly releases hydrogen from the fuel and produces the dehydrogenated organic liquid (DOL). The key to success in the HRM is the high surface area and stability of the catalyst. Asemblon has discovered and patented the right catalyst for this operation. To achieve the high surface area, Asemblon has developed several prototypes of hydrogen release units consisting of microchannels, packed bed made out of embedded nano-size catalysts on porous substrates and nanosprings. **Figure 2** shows one of these modules.

Figure 2. Asemblon Hydrogen Release Module.

(3) Spent Fuel Recovery Module

After the release of hydrogen, the DOL and hydrogen go into a spent fuel recovery module. Hydrogen gas and DOL are easily separated by their physical properties. If necessary, the hydrogen gas can be passed through a membrane for further purification. The separated hydrogen can then be directed to power internal combustion engines, turbines or fuel cells. The DOL from the spent fuel recovery module is directed to the dual-bladder gas tank where it is stored until it can be removed and transported to a remote site for catalytic hydrogenation.

(4) Hydrogenation Module

In the hydrogenation module, hydrogen is added to DOL to regenerate the original fuel. The art and chemistry of catalytic hydrogenation is well known. Asemblon is working with the experts in this field to find the best catalyst and its optimum condition to re-hydrogenate at high yield.

A "Well-to-Wheels" estimate for Asemblon's system is shown in **Figure 3**. This "Well-to-Wheels" estimate was done by considering the major energy inputs and outputs for HYDRNOL™ fuel from creation to use. The data in Figure 3 assume the hydrogen will be used in an internal combustion engine and shows an overall efficiency of 25%. This is significantly higher than the estimated efficiency of gasoline (14%).[16] If a fuel cell were used the efficiency would increase even more.[17]
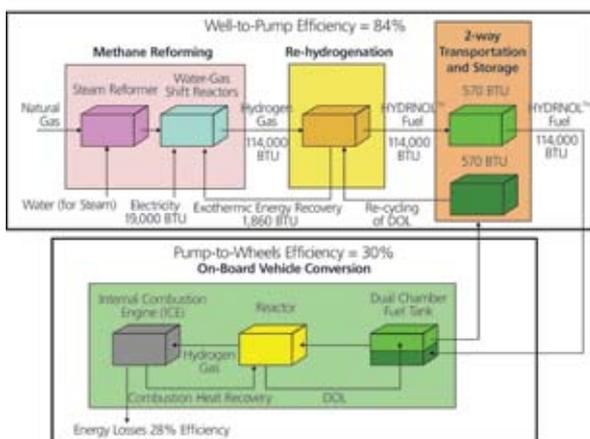
A Comparison of On-Board Hydrogen Storage Systems

The graphs in **Figure 4** compare four technologies for on-board vehicle storage of hydrogen. HYDRNOL™ compares favorably with compressed hydrogen, liquid hydrogen and hydrogen stored in metal hydrides on the basis of volume, weight and cost.

Not included in the cost factors are the much higher infrastructure costs associated with transporting and storing compressed and liquid hydrogen. Liquid hydrogen fueling is considered to be potentially dangerous, so expensive filling robots have been designed to eliminate the need for the consumer to fill the vehicle.

Generating hydrogen by steam methane reforming is relatively inexpensive. One kilogram of hydrogen currently costs $1.20. The same 1 kg of H_2 is equivalent to 1 gallon of gasoline. The cost to store and transport hydrogen more than triples its cost. Using HYDRNOL™ Fuel, 1 kg of hydrogen can be delivered for $2.50; comparable to gasoline (**Figure 5**).

Conclusion

The ability to store and transport hydrogen within a liquid carrier at standard temperatures and pressures provides many advantages over current hydrogen storage methods. The need for large, heavy storage tanks is eliminated. Major changes in the fueling infrastructure of the world are avoided. The risk for explosion is minimized since the hydrogen is stored within a molecule and not in its elemental form. HYDRNOL™ is such a liquid fuel. Due to the favorable properties, HYDRNOL™ presents opportunities not only in the transportation energy market, but also in stationary power generation and storage. The further development of HYDRNOL™ promises to revolutionize the future of energy storage, transportation and use.

Figure 3. Well-to-Wheels Estimate for Asemblon's HYDRNOL™ Fuel.

Figure 4. Comparison of On-Board Hydrogen Storage Systems

TO ORDER: Contact your local Sigma-Aldrich office (see back cover), call 1-800-325-3010 (USA), or visit sigma-aldrich.com/matsci.

sigma-aldrich.com

ALDRICH®

Comparative Cost to Deliver 1 kg of Hydrogen to a Vehicle

	Raw Cost of H$_2$ ($/kg)	Cost to Process H$_2$ ($/kg)	Cost to Transport H$_2$ ($/kg)	Cost of On-Site Storage of H$_2$ ($/kg)	Refueling Station Cost H$_2$ ($/kg)	Delivered Cost of H$_2$ ($/kg)
HYDRNOL™ Liquid	$1.20	$0.60 (Rehydrogenation)	$0.60 (2-way Transport)	$0.05 (Standard Temperature and Pressure)	$0.10	$2.50
Compressed Hydrogen	$1.20	$0.70 (Compression to 7,000 psi or 450 bar)	$0.70 (Pressurized Tanker)	$0.45 (High Pressure Storage Tanks)	$0.75	$3.80
Liquid Hydrogen	$1.20	$1.11 (Cryogenic Liquification)	$0.21 (Cryogenic Tanker)	$0.24 (Cryogenic Storage including boil-off losses)	$0.66	$3.42

Figure 5. Costs shown in U.S. dollars.

HYDRNOL™ as a carrier for hydrogen presents many advantages including:

1. Less flammable than gasoline or diesel
2. Can be stored at room temperature and normal atmospheric pressure
3. Can be converted on-board a vehicle as needed
4. Released hydrogen can be used for internal combustion engines and fuel cells
5. HYDRNOL™ can be shipped by standard methods
6. Current fueling infrastructure could be readily adapted for HYDRNOL™ use
7. Residuals can be recycled back to HYDRNOL™ by hydrogenation after use
8. Can be made from fossil fuels, refining waste and sour crude
9. Can be made from biomass via ethanol
10. Is not anticipated to have a significant environmental impact
11. Is cost effective when compared to traditional fuels
12. Can be used as a storage conversion device for electricity

References:

(1) http://hydrogenhighway.ca.gov/ (2) http://www.wired.com/news/autotech/0,2554,63145,00.html (3) http://www.greencarcongress.com/2005/05/california_roll.html (4) http://news.bbc.co.uk/1/hi/programmes/newsnight/archive/2208013.stm (5) http://www.afsa.org/fsj/dec03/sigfusson.pdf (6) http://physicsweb.org/articles/world/15/7/10/1 (7) http://www.hynor.no/pdf/engelsk-hynor-presentation.pdf (8) http://www.hynor.no/english (9) http://www.hydrogencarsnow.com/norway-hynor-project.htm (10) http://www1.eere.energy.gov/hydrogenandfuelcells/storage/current_technology.html (11) http://www.hydrogen.energy.gov/annual_review06_storage.html (12) Dillon, A. C.; Jones, K. M.; Bekkedahl, T. A.; Kiang, C. H.; Bethune, D. S.; Heben, M. J. *Nature*, **1997**, *386*, 377. (13) Ye, Y.; Ahn, C. C.; Witham, C.; Fultz, B.; Liu, J.; Rinzler, A. G.; Colbert, D.; Smith, K. A.; Smalley, R. E. *Applied Physics Letters* **1999**, *74*, 2307. (14) Bossel et. al., April 2003 report: "The Future of the Hydrogen Economy: Bright or bleak?" (15) http://www.hydrogen.energy.gov/pdfs/review06/st_9_cooper.pdf (16) http://www.exxonmobil.co.uk/files/pa/uk/FutureFuels_Oct2003.pdf (17) http://web.mit.edu/afs/athena.mit.edu/org/m/mecheng/fcp/about%20f%20cells.html

Substituted Carbazoles—Organic Materials with Potential Hydrogen Storage Applications

Name	Structure	Purity (%)	Prod. No.
Carbazole		95	**C5132-100G** **C5132-250G** **C5132-500G**
9-(2-Ethylhexyl)carbazole		97	**649511-1G** **649511-5G**
9-Ethylcarbazole		96.5	**E16600-5G** **E16600-100G** **E16600-500G**
9-Phenylcarbazole		>99	**262684-1G** **262684-5G**
9-Methylcarbazole		99	**325325-5G**
4,4'-Bis(*N*-carbazolyl)-1,1'-biphenyl		97	**660124-1G** **660124-5G**
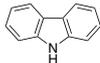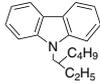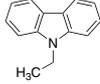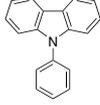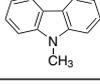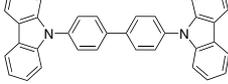
For questions, product data, or new product suggestions, please contact the Materials Science team at matsci@sial.com.

Organic Liquid Storage of Hydrogen

Order: 1.800.325.3010 Technical Service: 1.800.231.8327

ALDRICH®

The PCTPro-2000—The Ultimate Tool for Gas Sorption Analysis

Dr. Karl J. Gross, Hy-Energy, LLC.

Introduction

Gas sorption analysis is important in many fields of materials science and consumer product development. Some examples of current hot areas of technology involving gas-solid (or gas-liquid) interactions include the development of energy storage materials, improved catalysts for petrochemical processing, advanced pharmaceuticals and food industries.

At present, there is tremendous interest in the development of innovative materials for the transition to renewable energy. The science of gas sorption has become particularly critical in the advancement of materials for storing fuel gases such as hydrogen or natural gas, as well as for sequestration of greenhouse gases. Some exciting prospects for the chemical storage of gases include high-surface area and nanomaterials (graphitic carbons, CNT, zeolites, Metal-Organic-Framework MOFs).[1] In the field of hydrogen-storage, a host of novel materials are being developed including high-pressure metal-hydrides, light-weight complex hydrides, destabilized multi-component chemical hydrides and amides, and other cross-over materials such as ammonia borane encapsulated into mesoporous silica scaffolding.[2]

Of prime interest in the discovery of these and many other new materials is the characterization of gas absorption, adsorption and desorption kinetics, capacity, thermodynamic properties, as well as cycling performance of reversible materials. Also important is the ability to measure the tolerance of catalyst, chemicals, and consumer products to air, moisture and low-level contaminants. These wide-ranging requirements and the need to perform analysis at both a research and a production level (milligrams to kilograms) have driven the development of the PCTPro-2000, the ultimate tool for gas sorption analysis.

Careful analysis of physical and chemical interactions between gases and solids (or liquids) require extremely precise measurements. Several techniques are employed for gas sorption measurements the most common of these being gravimetric and volumetric methods. In volumetric methods the amount of gas sorbed is typically determined by a change in pressure within a calibrated volume containing the sample. In gravimetric methods, the amount of sorbed gas is determined by measuring the apparent mass change of the sample. In volumetric methods, the amount of gas sorbed is typically determined by a change in pressure within a calibrated volume containing the sample. We believe the volumetric method offers several distinct advantages over the gravimetric method, and of the volumetric instruments available, the PCTPro-2000 offers the best state-of-the-art measurements.

The Volumetric Method

One of the most common and versatile types of volumetric instruments is the Sieverts Apparatus. Simply put, a Sieverts Apparatus is an instrument containing two reservoirs of known volume connected by an isolation valve, as shown in **Figure 1**. The sample for measurement is loaded into the sample volume and the initial pressure reading is taken. For absorption the reservoir is filled with the sorption gas to a pre-determined pressure above that of the initial pressure in the sample volume. The isolation valve between the two volumes is opened and the gas is allowed to equilibrate between the reservoir and sample volume. By knowing the initial gas pressures and the volumes of the system, the quantities of absorbed or desorbed gas can be determined.
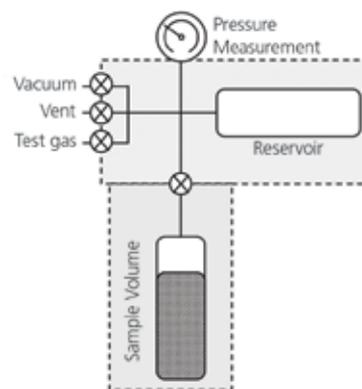
Figure 1. Schematic of a Sieverts Apparatus.

By applying the Sievert's approach to a system using a wide range of calibrated volumes, advanced pressure control, pressure measurements, and temperature control, it is possible to make a full suite of analyses with one device. Such analyses include:

Capacity

The total amount of gas absorbed or desorbed by a sample is pressure and temperature dependent and therefore requires precise measurements of both. In the volumetric method, capacity is directly related to pressure change. Small amounts of impurities in the test gas may be strongly absorbed by the sample. This can be very problematic in gravimetric methods as this uptake can cause significant weight change that might be misinterpreted. In the volumetric method, low levels of impurities may impact the performance of the material, but will not produce significant pressure changes.

Kinetics

Kinetics consists of the dynamic measurement of the change in moles of sorbed gas versus time. An advanced sorption analyzer should consist of multiple reservoirs with a wide range of volumes to match sample size and a wide range of sorption conditions associated with each different type of material. Additionally, sorption reactions generally involve significant endothermic or exothermic reactions. Heat transfer from the sample is a critical aspect of proper kinetics measurements. In a gravimetric instrument the sample is suspended from a microbalance that does not allow direct contact of temperature measuring probes or provide good heat transfer, limiting its usefulness.

TO ORDER: Contact your local Sigma-Aldrich office (see back cover), call 1-800-325-3010 (USA), or visit sigma-aldrich.com/matsci.

sigma-aldrich.com

ALDRICH®

Pressure-Composition Isotherms

Pressure-Composition Isotherms (PCT or PCI) is one of the most informative sorption measurements. The result is a plot of the equilibrium absorbed gas concentration in the material as a function of pressure and temperature.

The volumetric approach to PCI measurements consists of adding (or removing) gas to the sample volume in a small dose from one of the calibrated reservoirs and waiting for the resulting gas/solid equilibrium. The PCI curve is produced from the concentration of gas sorbed and the final pressure of each dose in a series of many doses that either increase (absorption) or decrease (desorption) in pressure. This is essentially a gas titration process.

The PCI plot will typically show an equilibrium plateau associated with the co-existence of the remaining unreacted material and the gas-reacted material, thus providing a complete phase diagram. For example, metal hydride materials that reversibly react with hydrogen show a well-defined plateau between the solid solution α-phase, where hydrogen is randomly dissolved within the solid matrix, and the β-phase, where hydrogen is in distinct structural sites and has bonded to the host solid material.[3] In addition, precise dosing PCI measurements can provide detailed information on the presence of crystal structure changes, new phases and sorption kinetics as a function of gas concentration.

The PCTPro-2000 makes these measurements easy and has been used extensively in research on complex hydrides such as Ti-catalyzed alanates. Work by researchers at the Max Planck Institute for Coal Research in Germany, investigated the kinetic and thermodynamic effects of varying doping levels of Ti on $NaAlH_4$.[4] **Figure 2** shows a 160 °C PCT curves for 6 different mole-% doping levels of Ti.
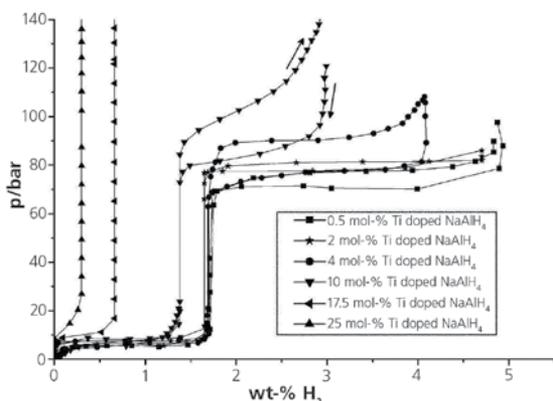
Figure 2. PCT curves for 0.5, 2, 4, 10, 17.5 and 25 mol% Ti doped $NaAlH_4$ at 160 °C. Taken from Ref. 4.

With the PCTPro-2000, each gas dose can be chosen to be equi-molar and range from extremely small to very large doses (0.1 micro-mole to 10 moles of gas). Now, thanks to the MicroDoser attachment for the PCTPro-2000, it is also possible to extend the full suite of measurement capabilities from very small samples down to milligrams, previously the one real advantage of the gravimetric instruments.

Thermodynamic measurements

The enthalpy and entropy of sorption can be precisely determined by a series of PCI measurements at different temperatures. This results in the van't Hoff relationship:

$$\ln P = \Delta H/RT - \Delta S/R$$

where P is the equilibrium gas pressure, T the absolute temperature, R the gas content, ΔH the reaction enthalpy and ΔS the reaction entropy.[5] **Figure 3** shows PCT measurements for $LaNi_5$, a classic intermetallic hydride, at six temperatures and the van't Hoff plot showing the temperature/pressure relationship.[6] The PCTPro-2000 instrument enables the direct determination of ΔH and ΔS in a single measurement, thus reducing the measurement time dramatically.
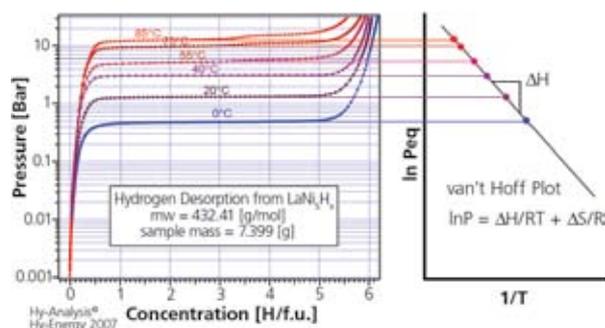
Figure 3. PCT curves and van't Hoff plot for $LaNi_5$.[3]

Materials Performance Measurements

In addition to the fundamental mechanisms of gas-solid and gas-liquid interactions, Sievert's instruments are ideal for collecting important material performance data. For example, by making cycle life measurements and catalytic measurements with introduced impurities in the sorption gas, the tolerance of the sample to poisoning can be determined. This information can be very valuable when considering a material's potential for commercial applications.

Versatility

The biggest advantage of the PCTPro-2000 over a gravimetric system is that the sorption measurement is independent of the sample holder design. Unlike gravimetric systems where the sample is restricted to being placed on the balance arm or lever, the sample holder of a volumetric instrument can be of any size, shape, material, position, and location. This makes the volumetric device ideal for simultaneous secondary measurements such as in situ XRD, IR, neutron diffraction, spectrometry, thermal conductivity, electrical conductivity, and many more. An example of the simultaneous controlled deuteration and neutron diffraction of $CeMn_{1.5}Al_{0.5}$ is shown in **Figure 4a** and **b**. The possibilities for in situ measurement of other materials properties are unlimited.
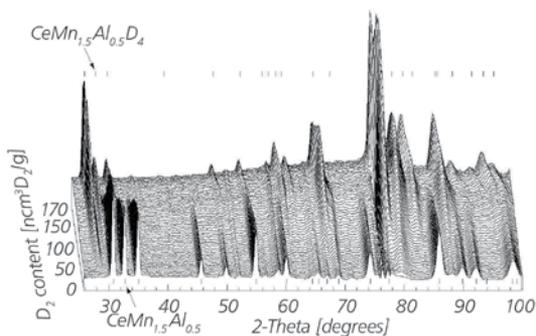
Figure 4a. In situ XRD measurements; instrument D2B-ILL Grenoble.[7]
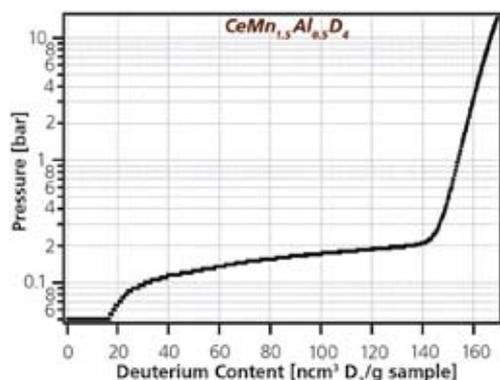
Figure 4b. Deuterium capacity correlated with neutron diffraction patterns.

References:

(1) Eddaoudi, M.; Kim J; Rosi, N.; Vodak, D.; Wachter, J.; O'Keeffe, M.; Yaghi, O. M. *Science* **2002**, *295*. 469. (2) Gutowska, A.; Li, L.; Shin, Y.; Wang, C. M.; Li, X. S.; Linehan, J. C.; Smith, R. S.; Kay, B. D.; Schmid, B.; Shaw, W.; Gutowski, M.; Autrey, T. *Angew. Chem. Int. Ed.* **2005**, *44*, 3578. (3) Schlapbach, L. *Topics Appl. Phys.*, **1988**, *63*, 10. (4) Struekens G.; Bogdanovič, B.; Felderhoff, M.; Schüth, F.; *Phys. Chem. Chem. Phys.*, **2006**, *8*, 2889. (5) Sandrock, G. "*State-of-the-Art Review of Hydrogen Storage in Reversible Metal Hydrides for Military Fuel Cell Applications,*" ONR Report, DTIC #AD-A328073, p. 10. (6) Measurements made at Hy-Energy by Karl J. Gross on a sample of LaNi$_5$. (7) Gross, K. J.; Chartouni, D.; Fauth, F. *J. Alloys Comp.* **2000**, *306*, 203. Note: K. Gross in situ neutron diffraction measurements.

Reference Kit for Hydrogen Storage—686115–1KT

Materials included in the kit are designed to be used with the PCTPro-2000 System. They can also be used for demonstration purposes and as standards during the development of novel hydrogen storage and battery materials.

Name	Chem. composition	Hydrogen storage capacity, wt %	Equilibrium pressure plateau	Prod. No.
Lanthanum Nickel Alloy, LaNi$_5$	LaNi$_5$	~1.4 (25 °C)	~2 bar (25 °C)	**685933-10G**
Lanthanum Nickel Alloy, LaNi$_{4.5}$Co$_{0.5}$	LaNi$_{4.5}$Co$_{0.5}$	~1.4 (25 °C)	< 0.5 bar (25 °C)	**685968-10G**
Mischmetal Nickel Alloy, (Ce, La,Nd, Pr)Ni$_5$	MmNi$_5$ Mm: La: 20–27%; Ce: 48–56%; Pr: 4–7%; Nd: 12–20%	~1.4 (25 °C)	~10 bar (25 °C)	**685976-10G**
Titanium Manganese Alloy, TiMn$_2$, Alloy 5800	Ti$_{0.98}$Zr$_{0.02}$V$_{0.43}$Fe$_{0.09}$Cr$_{0.05}$Mn$_{1.5}$	~1.6 (25 °C)	~10 bar (25 °C)	**685941-10G**

For more information about these and other related materials, please visit **sigma-aldrich.com/hydrogen**.

Gas Sorption Analysis Tool

Nuclear Magnetic Resonance Studies of Hydrogen Storage Materials

Dr. Robert C. Bowman, Jr. and Dr. Son-Jong Hwang
California Institute of Technology

Introduction

Solid-state nuclear magnetic resonance (NMR) methods have been used to characterize metal hydrides and other hydrogen storage materials for over fifty years. Until recently, attention was usually focused on assessing structural properties, electronic parameters, and diffusion behavior of the hydride phases of metals and alloys using mostly transient NMR techniques or low-resolution spectroscopy.[1–3] This interest was stimulated by the excellent resonance properties of the three common hydrogen isotopes (i.e., ^{1}H, ^{2}D, and ^{3}T) and some other host nuclei (e.g., ^{23}Na, ^{45}Sc, ^{51}V, ^{89}Y, ^{93}Nb, and ^{139}La), which allowed detailed evaluation of local interactions between hydrogen and metal atoms, thus complementing diffraction and thermochemical measurements. In particular, the NMR relaxation times are extremely useful to assess diffusion processes over very wide ranges of hydrogen mobility in crystalline and amorphous phases.[1–3]

In order to achieve the challenging weight and volume goals set for the hydrogen storage systems for automotive applications by the U.S. Department of Energy,[4] only the lightest elements (i.e., Li, B, C, N, Na, Mg, Al, Si) can be considered as a basis for such systems. The development and evaluation of hydride-based materials combining various light metal hydrides and transition metal catalysts are the focus of research efforts by numerous international research groups. By implementing advanced solid-state NMR techniques,[5] such as Magic Angle Spinning (MAS), and multi-quantum (MQ) MAS NMR in addition to traditional measurements of nuclear relaxation times,[1–3] hydride phases of light elements can be investigated more efficiently. Solid-state NMR techniques also offer a better insight into complicated relationships between various processes accompanying the formation of hydride phases and their transformations, including reaction kinetics, reversibility, and the role of catalysts.

To illustrate the current state of solid-state NMR research in the area of hydrogen storage, we will discuss some recent examples typical for the field.

Aluminum-Hydrogen Systems

With hydrogen content of about 10 wt%, alane (i.e., AlH_3) and alkali metal alanates (i.e., $LiAlH_4$ and $NaAlH_4$) are being widely investigated as potential hydrogen storage materials. Although some additives such as Ti-compounds can substantially enhance the reaction rates for alanates[6] and alane based materials,[7] significant issues remain with respect to the reversibility and stability of these hydride phases. Increasingly, solid-state NMR techniques are being used to evaluate phase compositions and transformations in alanates[8–15] and alane.[16–18]

Figure 1 presents static and ^{1}H MAS NMR spectra of α-AlH$_3$ obtained at the Caltech Solid-State NMR Facility.
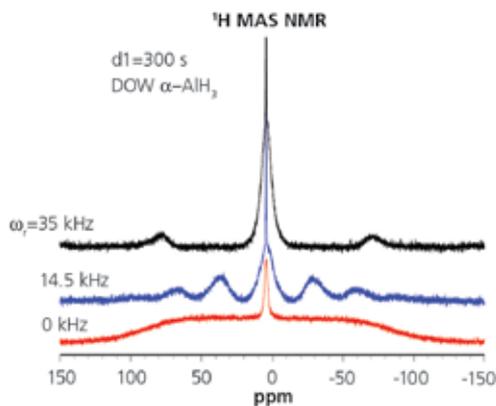
Figure 1. Static and ^{1}H MAS NMR spectra of α phase aluminum hydride (α-AlH$_3$) obtained at the resonance frequency of 500.23 MHz. (bottom) static (0 kHz) d1= 300 s, (middle) MAS (14.5 kHz), d1=300 s, (top) MAS (35 kHz), d1=300 s, where d1 is the repetition delay time during signal averaging.

Static NMR spectra of solids often reveal featureless broadening due to anisotropic interactions between atoms in the solid-state. Such interactions include dipole-dipole couplings, chemical shift anisotropies and quadrupole couplings for nuclei with I>1/2. High-speed (i.e., > 5 kHz) rotation of a sample aligned at the specific "magic angle" of 54.7° with respect to the direction of the external magnetic field averages out most of these broadening sources to yield highly resolved narrow and isotropic lines.[5] In Figure 1, the very broad component in the static spectrum (0 kHz) is from the immobile protons in the hydride phase while a sharper peak is attributed[17] to the molecules of gaseous hydrogen trapped in the solid (~4% of the total hydrogen content). Although MAS narrows the broad peak, intense residual spinning side bands are still observed in the spectrum even at the very high rotation speed of 35 kHz. These side bands are the result of very strong dipolar interactions that cannot be removed completely.

A series of spinning side bands are also observed in the ^{27}Al MAS NMR spectra shown in **Figure 2**.
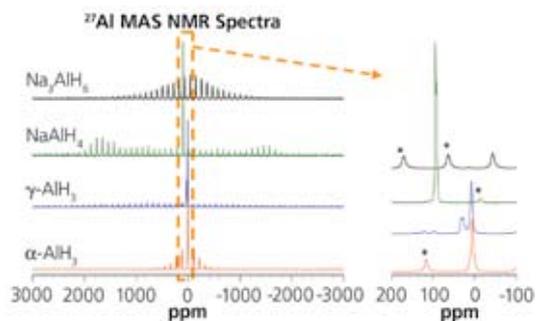
Figure 2. ^{27}Al MAS NMR spectra of α and γ phases of AlH$_3$, NaAlH$_4$ and Na$_3$AlH$_6$ obtained at the resonance frequency 130.35 MHz with strong ^{1}H decoupling.

Solid-State NMR of Metal Hydrides

Order: 1.800.325.3010 Technical Service: 1.800.231.8327

ALDRICH®

They arise from various quadrupolar interactions[5] in α and γ-AlH$_3$, or other aluminum-based hydrides. However, while the intrinsic small range of chemical shifts for protons along with large residual dipolar interactions limits the information that can be obtained from even fast-spinning ^{1}H MAS NMR spectra, the ^{27}Al MAS NMR is capable of providing an additional insight into the local symmetry and bonding in the material. The isotropic chemical shifts (δ_{iso}) and quadrupolar parameters[5] C$_Q$ and η for several different AlH$_3$ and alanate phases are summarized in **Table 1**. It is easy to see that ^{27}Al MAS NMR technique allows for a clear and distinct identification of tetrahedral and octahedral coordination sites in various types of aluminum-based hydride materials.

Table 1. The peak shifts and quadrupole coupling parameters for ^{27}Al spectra from AlH$_3$, the Li and Na alanate phases, and Al metal.

Phase	Al site	δ_{iso} (ppm)	C$_Q$ (MHz)[a]	η[b]	Reference
α-AlH$_3$	AlH$_6$	5.8	0.25	0.1	17,18
β-AlH$_3$	AlH$_6$	21.5	0.38	0.49	17,18
γ-AlH$_3$	AlH$_6$-I	10.9	2.9	0.58	17,18
	AlH$_6$-II	36.0	4.0	0.02	
LiAlH$_4$	AlH$_4^-$	103.8	3.9	0.24	12
Li$_3$AlH$_6$	AlH$_6^{-3}$	−33.7	1.4	0.02	12
NaAlH$_4$	AlH$_4^-$	101	2.95	0	8
Na$_3$AlH$_6$	AlH$_6^{-3}$	−42.7	–	–	11
Al metal	Al$_6$	1641	–	–	14

[a]C$_Q$ is the quadrupole coupling constant.
[b]η is the asymmetry parameter.

^{27}Al MAS NMR also allows detection of aluminum metal and its oxide phases in aluminum-based hydrides during their processing and monitoring both chemical processes and contaminations.[8–18] For example, oxide phases[14] in α-AlH$_3$ can be clearly identified in the spectrum shown in **Figure 3**.
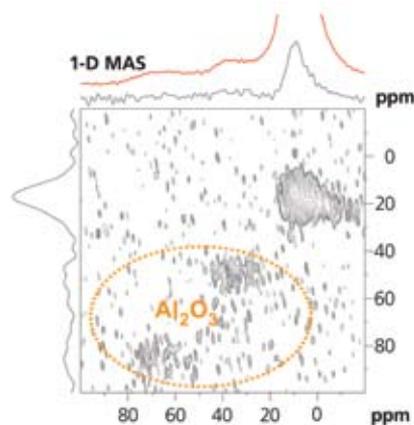
Figure 3. Two-Dimensional (2D) MQMAS ^{27}Al spectrum of α-AlH$_3$ (ω_r=35 kHz) shows two weaker peaks at ~40 ppm and ~65 ppm from 5-fold and 6-fold Al-O sites in addition to the peak at 6 ppm from the hydride.

NMR analysis of quadrupole nuclei such as ^{27}Al, ^{23}Na, ^{11}B, etc. can benefit from the MQMAS NMR technique developed by Frydman[19] and others[20,21] for obtaining highly resolved isotropic line components free of quadrupole interactions. The MQMAS method is especially appropriate for quadrupole nuclei because it eliminates the second order quadrupole interactions, which cannot be removed by the MAS NMR alone. Figure 3 shows an example of ^{27}Al 2D MQMAS NMR spectrum that reveals the presence of oxide phases, which

the corresponding 1D ^{27}Al MAS NMR spectrum alone cannot identify unambiguously. It is worth noting that recently Herberg, et al.[14] have successfully used ^{27}Al MQMAS to evaluate Al-oxide phases in Ti-doped sodium alanate.

MAS NMR Spectroscopy of Deuterides

Information about the specific locations and symmetries of hydrogen in a hydrogen storage material is highly desirable for determining the detailed structures and dynamic behavior of the hydride phase. Unfortunately, due to narrow ranges of chemical shifts and extensive residual dipolar proton-proton interactions, ^{1}H MAS NMR is not always a best solution for such investigations. However, dipolar broadening as well as quadrupolar contributions can be significantly reduced or even eliminated for the deuterons (^{2}D) in deuteride phases, which makes it possible to observe local symmetries and multiple site occupancies directly.[22–24]

Figure 4 presents the ^{2}D MAS NMR spectra of two different ZrNiD$_x$ phases with two distinctly different lattice sites for each phase.[23] These NMR results are strongly supported by neutron powder diffraction studies of the β-ZrNiD$_{0.88}$,[25] which, contrary to the prior assignment, also reveal two locations for D-atoms. This allows for a better understanding[23] of diffusion processes in both phases of ZrNiD$_{0.88}$.
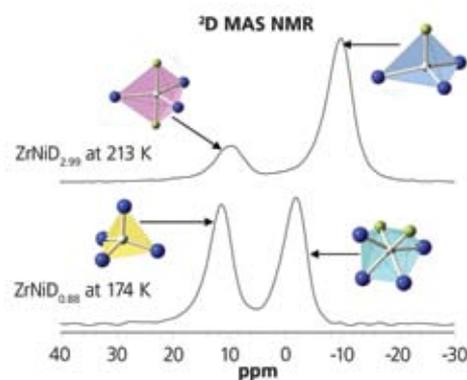
Figure 4. Rigid-lattice ^{2}D MAS NMR spectra (f$_o$=76.79 MHz) for the γ-ZrNiD$_{2.99}$ (upper) and the β-ZrNiD$_{0.88}$ (lower). Spinning sidebands are not shown in both spectra. The fits to these spectra yield two distinct resonances for each phase that correspond to the indicated D sites as described in Ref. 23.

In another example, Adolphi and co-workers have used ^{2}D MAS NMR techniques to differentiate the occupancy and mobility of deuterons in the tetrahedral and octahedral sites in YD$_x$ phases and showed that this approach can be used on different classes of deuterides.[22,24]

Summary

A few examples showing the versatility of multinuclear and multidimensional NMR to evaluate the structure and behavior of metal hydrides were presented in this short review. Additionally, nuclear relaxation times have been used[1–3] to characterize diffusion processes and mechanisms for many classes of metal hydrogen systems. Recent studies, describing diffusion assessments by means of relaxation times measurements, include reports on LaNi$_5$H$_x$,[24] Mg-based hydrides,[24] NaAlH$_4$,[26] and the ZrNiH$_x$/ZrNiD$_x$ phases.[27] Thus, various NMR approaches can be applied to various hydrogen storage media being investigated now and coming into the picture in the future. Immediate candidates include metal

alanates, borohydrides, metal amides, and destabilized lithium and magnesium hydrides.[28] The combinations of MAS NMR and MQMAS NMR techniques should provide much greater insights into the local structures, bonding, and dynamics of these materials.

References:

(1) Cotts, R. M. in *Hydrogen in Metals I: Basic Properties*; Alefeld, G.; J. Volkl (Eds.); Springer: Berlin-Heidelberg, **1978**; p. 227. (2) Richter, D.; Hempelmann, R.; Bowman, Jr., R. C. in *Hydrogen in Intermetallic Compounds II – Surfaces and Dynamic Properties, Applications*, Schlapbach, L. (Ed.); Springer-Verlag: Berlin, **1992**; p. 97. (3) Barnes, R. G. in *Hydrogen in Metals III: Properties and Applications*; Wipf, H. (Ed.); Springer-Verlag: Berlin; **1997**; p. 93. (4) Chandra, D.; Reilly, J. J.; Chellappa, R. *Journal of Metals (JOM)* **2006**, *58*, 26. (5) MacKenzie, K. J. D.; Smith, M. E. *Multinuclear Solid-State NMR of Inorganic Materials*; Pergamon: Amsterdam, **2002**. (6) Bogdanovič, B.; Sandrock, G. *MRS Bulletin* **2002**, *27*, 712. (7) Graetz, J.; Reilly, J. J. *J. Phys. Chem. B* **2005**, *109*, 22181. (8) Tarasov, V. P.; Bakum, S. I.; Privalov, V. I.; Muravlev, Yu. B; Samoilenko, A. A. *Russ. J. Inorg. Chem.* **1996**, *41*, 1104. (9) Tarasov, V. P.; Bakum, S. I.; Kuznetsova, S. F. *Russ. J. Inorg. Chem.* **1997**, *42*, 694. (10) Balema, V. P.; Wiench, J. W.; Dennis, K. W.; Pruski, M.; Pecharsky, V. K. *J. Alloys Compd.* **2001**, *329*, 108. (11) Bogdanovič, B.; Felderhoff, M.; Germann, M.; Hartel, M.; Pommerin, A.; Schuth, F.; Weidenthaler, C.; Zibrowius, B. *J. Alloys Compd.* **2003**, *350*, 246. (12) Wiench, J. W.; Balema, V. P.; Pecharsky, V. K.; Pruski, M. *J. Solid State Chem.* **2004**, *177*, 648. (13) Majzoub, E. H.; Herberg, J. L.; Stumpf, R.; Spangler, S.; Maxwell, R. S. *J. Alloys Compd.* **2005**, *394*, 265. (14) Herberg, J. L.; Maxwell, R. S.; Majzoub, E. H. *J. Alloys Compd.* **2006**, *417*, 39. (15) Mamatha, M.; Bogdanovič, B.; Felderhoff, M.; Pommerin, A.; Schmidt, W.; Schuth, F.; Weidenthaler, C. *J. Alloys Compd.* **2006**, *407*, 78. (16) Zogal, O. J.; Stalinski, B.; Idziak, S. *Z. Physik. Chem. N.F.* **1985**, *145*, 167. (17) Hwang, S.-J.; Bowman, R. C.; Graetz, J. Reilly, J. J. In: Wang, J. C. F.; Tumas, W.; Rougier, A.; Heben, M. J.; Akiba, E. (Eds), *Hydrogen Storage Materials,* Mater. Res. Soc. Symp. Proc. Warrendale, PA, **2006**, Vol 927E, 0927-EE03-03. (18) Hwang, S.-J.; Bowman, Jr., R. C.; Reilly, J. J.; Langley, W.; Jensen, C. M. *J. Alloys Compd.* **2007**, in press. (19) Frydman, L.; Harwood, J. S. *J. Am. Chem. Soc.* **1995**, *117*, 5367. (20) Amoureux, J. P.; Fernandez, C. *Solid State NMR* **1998**, *10*, 211. (21) Amoureux, J. P.; Pruski, M. In: Grant, D. M; Harris, R. K. (Eds) *Encyclopedia of NMR*, John Wiley & Sons: Chichester, UK, **2002**, *9*, 226. (22) Adolphi, N. L.; Balbach, J. J.; Conradi, M. S.; Markert, J. T.; Cotts, R. M.; Vajda, P. *Phys. Rev. B* **1996**, *53*, 15054. (23) Bowman, Jr., R. C.; Adolphi, N. L.; Hwang, S.-J.; Kulleck, J. G.; Udovic, T. J.; Huang, Q.; Wu, H. *Phys. Rev. B* **2006**, *74*, 184109. (24) Conradi, M. S.; Mendenhall, M. P.; Ivancic, T. M.; Carl, E. A; Browning, C. D.; Notten, P. H. L.; Kalisvaart, W. P.; Magusin, P. C. M. M.; Bowman, Jr., R. C.; Hwang, S.-J.; Adolphi, N. L. *J. Alloys Compd.* **2007** (in Press). (25) Wu, H.; Zhou, W.; Udovic, T. J.; Rush, J. J.; Yildirim, T.; Huang, Q.; Bowman, Jr., R. C. *Phys. Rev. B* **2007**, *75*, 064105. (26) Majer, G.; Stanik, E.; Valiente Banuet, L. E.; Grinberg, F.; Kircher, O.; Fichtner, M. *J. Alloys Compd.* **2005**, *738*, 404. (27) Browning, C. D.; Ivancic, T. M.; Bowman Jr., R. C.; Conradi, M. S. *Phys. Rev. B* **2006**, *73*, 134113. (28) Vajo, J. J.; Mertens, F.; Ahn, C. C.; Bowman, Jr., R. C.; and Fultz, B. *J. Phys. Chem. B* **2004**, *108*, 13977.

Isotope-Enriched Materials for Hydrogen Storage Research

Name	Mol. Formula	Purity	Prod. No.
Ammonia-d$_3$	ND$_3$	99% D	**422975-10L** **422975-25L**
Ammonia-^{15}N,d$_3$	^{15}ND$_3$	99 atom % D, 98 atom % ^{15}N	**485373-1L**
Borane-d$_3$-THF complex	D$_3$B–O(CH$_2$)$_4$	97.5 atom % D	**667714-1ML** **667714-5X1ML**
Deuterium hydride	D–H	96 atom % D	**488690-1L**
Deuterium	D$_2$	99.96 atom % D	**368407-10L** **368407-25L**
Deuterium	D$_2$	99.9 atom % D	**617474-25L**
Lithium aluminum deuteride	LiAlD$_4$	98 atom % D	**193100-1G** **193100-5G**
Lithium deuteride	LiD	98 atom % D	**555363-1G** **555363-10G**
Lithium borodeuteride	LiBD$_4$	98 atom % D	**685917-500MG**
Sodium borodeuteride	NaBD$_4$	98 atom % D	**205591-1G** **205591-5G**
Sodium borohydride, ^{11}B	Na ^{11}BH$_4$	98+ %(assay), 99 atom % ^{11}B	**679623-1G** **679623-10G**
Trimethyl borate-^{11}B	^{11}B(OCH$_3$)$_3$	98+ %(assay), 99 atom % ^{11}B	**427616-1G**
Tributyl borate-^{10}B	^{10}B(OCH$_3$)$_3$	98 atom % ^{10}B	**427640-1G** **427640-10G**

For details visit **sigma-aldrich.com/hydrogen**.

Solid-State NMR of Metal Hydrides

ALDRICH®

Argentina
SIGMA-ALDRICH DE ARGENTINA S.A.
Free Tel: 0810 888 7446
Tel: (+54) 11 4556 1472
Fax: (+54) 11 4552 1698

Australia
SIGMA-ALDRICH PTY LTD.
Free Tel: 1800 800 097
Free Fax: 1800 800 096
Tel: (+61) 2 9841 0555
Fax: (+61) 2 9841 0500

Austria
SIGMA-ALDRICH HANDELS GmbH
Tel: (+43) 1 605 81 10
Fax: (+43) 1 605 81 20

Belgium
SIGMA-ALDRICH NV/SA.
Free Tel: 0800 14747
Free Fax: 0800 14745
Tel: (+32) 3 899 13 01
Fax: (+32) 3 899 13 11

Brazil
SIGMA-ALDRICH BRASIL LTDA.
Free Tel: 0800 701 7425
Tel: (+55) 11 3732 3100
Fax: (+55) 11 5522 9895

Canada
SIGMA-ALDRICH CANADA LTD.
Free Tel: 1800 565 1400
Free Fax: 1800 265 3858
Tel: (+1) 905 829 9500
Fax: (+1) 905 829 9292

China
SIGMA-ALDRICH (SHANGHAI)
TRADING CO. LTD.
Free Tel: 800 819 3336
Tel: (+86) 21 6141 5566
Fax: (+86) 21 6141 5567

Czech Republic
SIGMA-ALDRICH S.R.O.
Tel: (+420) 246 003 200
Fax: (+420) 246 003 291

Denmark
SIGMA-ALDRICH DENMARK A/S
Tel: (+45) 43 56 59 10
Fax: (+45) 43 56 59 05

Finland
SIGMA-ALDRICH FINLAND OY
Tel: (+358) 9 350 9250
Fax: (+358) 9 350 92555

France
SIGMA-ALDRICH CHIMIE S.à.r.l.
Free Tel: 0800 211 408
Free Fax: 0800 031 052
Tel: (+33) 474 82 28 00
Fax: (+33) 474 95 68 08

Germany
SIGMA-ALDRICH CHEMIE GmbH
Free Tel: 0800 51 55 000
Free Fax: 0800 64 90 000
Tel: (+49) 89 6513 0
Fax: (+49) 89 6513 1160

Greece
SIGMA-ALDRICH (O.M.) LTD.
Tel: (+30) 210 994 8010
Fax: (+30) 210 994 3831

Hungary
SIGMA-ALDRICH Kft
Ingyenes zöld telefon: 06 80 355 355
Ingyenes zöld fax: 06 80 344 344
Tel: (+36) 1 235 9055
Fax: (+36) 1 235 9050

India
SIGMA-ALDRICH CHEMICALS
PRIVATE LIMITED
Telephone
Bangalore: (+91) 80 6621 9600
New Delhi: (+91) 11 4165 4255
Mumbai: (+91) 22 2570 2364
Hyderabad: (+91) 40 6684 5488
Fax
Bangalore: (+91) 80 6621 9650
New Delhi: (+91) 11 4165 4266
Mumbai: (+91) 22 2579 7589
Hyderabad: (+91) 40 6684 5466

Ireland
SIGMA-ALDRICH IRELAND LTD.
Free Tel: 1800 200 888
Free Fax: 1800 600 222
Tel: (+353) 1 404 1900
Fax: (+353) 1 404 1910

Israel
SIGMA-ALDRICH ISRAEL LTD.
Free Tel: 1 800 70 2222
Tel: (+972) 8 948 4100
Fax: (+972) 8 948 4200

Italy
SIGMA-ALDRICH S.r.l.
Numero Verde: 800 827018
Tel: (+39) 02 3341 7310
Fax: (+39) 02 3801 0737

Japan
SIGMA-ALDRICH JAPAN K.K.
Tokyo Tel: (+81) 3 5796 7300
Tokyo Fax: (+81) 3 5796 7315

Korea
SIGMA-ALDRICH KOREA
Free Tel: (+82) 80 023 7111
Free Fax: (+82) 80 023 8111
Tel: (+82) 31 329 9000
Fax: (+82) 31 329 9090

Malaysia
SIGMA-ALDRICH (M) SDN. BHD
Tel: (+60) 3 5635 3321
Fax: (+60) 3 5635 4116

Mexico
SIGMA-ALDRICH QUÍMICA, S.A. de C.V.
Free Tel: 01 800 007 5300
Free Fax: 01 800 712 9920
Tel: 52 722 276 1600
Fax: 52 722 276 1601

The Netherlands
SIGMA-ALDRICH CHEMIE BV
Free Tel: 0800 022 9088
Free Fax: 0800 022 9089
Tel: (+31) 78 620 5411
Fax: (+31) 78 620 5421

New Zealand
SIGMA-ALDRICH NEW ZEALAND LTD.
Free Tel: 0800 936 666
Free Fax: 0800 937 777
Tel: (+61) 2 9841 0555
Fax: (+61) 2 9841 0500

Norway
SIGMA-ALDRICH NORWAY AS
Tel: (+47) 23 17 60 60
Fax: (+47) 23 17 60 50

Poland
SIGMA-ALDRICH Sp. z o.o.
Tel: (+48) 61 829 01 00
Fax: (+48) 61 829 01 20

Portugal
SIGMA-ALDRICH QUÍMICA, S.A.
Free Tel: 800 202 180
Free Fax: 800 202 178
Tel: (+351) 21 924 2555
Fax: (+351) 21 924 2610

Russia
SIGMA-ALDRICH RUS, LLC
Tel: +7 (495) 621 6037
Fax: +7 (495) 621 5923

Singapore
SIGMA-ALDRICH PTE. LTD.
Tel: (+65) 6779 1200
Fax: (+65) 6779 1822

South Africa
SIGMA-ALDRICH
SOUTH AFRICA (PTY) LTD.
Free Tel: 0800 1100 75
Free Fax: 0800 1100 79
Tel: (+27) 11 979 1188
Fax: (+27) 11 979 1119

Spain
SIGMA-ALDRICH QUÍMICA, S.A.
Free Tel: 900 101 376
Free Fax: 900 102 028
Tel: (+34) 91 661 99 77
Fax: (+34) 91 661 96 42

Sweden
SIGMA-ALDRICH SWEDEN AB
Tel: (+46) 8 742 4200
Fax: (+46) 8 742 4243

Switzerland
SIGMA-ALDRICH CHEMIE GmbH
Free Tel: 0800 80 00 80
Free Fax: 0800 80 00 81
Tel: (+41) 81 755 2828
Fax: (+41) 81 755 2815

United Kingdom
SIGMA-ALDRICH COMPANY LTD.
Free Tel: 0800 717 181
Free Fax: 0800 378 785
Tel: (+44) 1747 833 000
Fax: (+44) 1747 833 313
SAFC (UK) Free Tel: 0800 71 71 17

United States
SIGMA-ALDRICH
P.O. Box 14508
St. Louis, Missouri 63178
Toll-Free: 800 325 3010
Toll-Free Fax: 800 325 5052
Call Collect: (+1) 314 771 5750
Tel: (+1) 314 771 5765
Fax: (+1) 314 771 5757

Internet
sigma-aldrich.com

World Headquarters
3050 Spruce St., St. Louis, MO 63103
(314) 771-5765
sigma-aldrich.com

Order/Customer Service (800) 325-3010 • Fax (800) 325-5052
Technical Service (800) 325-5832 • sigma-aldrich.com/techservice
Development/Bulk Manufacturing Inquiries SAFC (800) 244-1173

SIGMA-ALDRICH

*Accelerating Customers' Success
through Leadership in Life Science,
High Technology and Service*

The SIGMA-ALDRICH Group

SIGMA · ALDRICH · Fluka · Riedel-de Haën · SAFC · SUPELCO · ISOTEC

JMG
02359-503403
0047

SIGMA-ALDRICH™
3050 Spruce Street • St. Louis, MO 63103 USA